



ISAS - INTERNATIONAL SCHOOL FOR ADVANCED STUDIES

T E S I

DIPLOMA DI PERFEZIONAMENTO

DI

"DOCTOR PHILOSOPHIAE"

THE GRAVITATIONAL COLLAPSE AND THE ISSUE OF FINAL STATE

CANDIDATO:

Dott. Yu Yungiang

RELATORE:

Prof. F. de FELICE

**SISSA - SCUOLA
INTERNAZIONALE
SUPERIORE
DI STUDI AVANZATI**

TRIESTE
Strada Costiera 11

Anno Accademico 1981/1982

TRIESTE

The Gravitational Collapse

and

The Issue of Final State

by Yu Yunqiang

A thesis submitted for
the attainment of the
degree of Philosophy Doctor
at the S.I.S.S.A. Trieste

September 1982

ABSTRACT

The following thesis titled with "The Gravitational Collapse and the Issue of Final State" is intended to prepare the way for a full understanding of the fate of collapsing objects which can be, in general, both rotating and charged.

We have paid more attention to the rotating but uncharged cases. For these cases, the ratio of specific angular momentum a to mass m (both in $c=G=1$ unit system) is used as a rotational parameter. We first show that the cores of main-sequence stars have the value of ratio a/m in the range of 10 to 100; on the other hand, observed neutron stars have very small value of a/m which is in the range 10^{-2} to 10^{-4} . Possible mechanisms for reducing a/m during the evolution have been analysed in Chapter II. The most interesting result is that a newly formed neutron star probably has the value of a/m of the order of 1. Several evidences and relevant facts have been pointed out in Chapters II and III. The interesting point is that the value of 1 is just the critical value of a/m for forming an event horizon in the infinitely collapsing cases.

In order to estimate the a/m loss due to the gravitational radiation during collapse, a fast rotating ellipsoid model has been worked out

in Chapter III. It is shown that in favourable cases, one may expect the value of a/m to be reduced from (5-10) to 1. If the initial a/m is larger than (5-10), the collapsing object will probably be fragmented during collapse.

The gravitational trapping effect of neutrinos in condensed objects is considered in Chapter IV. We point out a) for massive neutrinos, the gravitational trapping effect is much stronger than that of massless neutrinos; b) even electronic neutrino are massive, the gravitational trapping effect alone is not strong enough to have significant influence to the collapsing process.

Finally, the collapse of a charged but non-rotating star is studied in Chapter V. Interesting results appear in the $Q > m$ case. It is shown that the collapse of a charged star with $Q > m$ would lead to form a vibrating dense star rather than a naked singularity. Optically, a quasi-stationary redshift will be seen from such an object. There is a notable point that the redshift can be large enough to confuse with a cosmological redshift of a distant galaxy, if the charge Q is nearly equal to the mass m .

CONTENTS

CHAPTER I	A SHORT REVIEW OF THE PROBLEM OF GRAVITATIONAL COLLAPSE AND FINAL STATES	
1.1	Introduction	1
1.2	The Evolution of Massive Stars before Collapse	5
1.3	Gravitational Collapse of Stellar Cores	9
1.4	Final States after Collapse	13
	References	20
CHAPTER II	STELLAR ROTATION AND NEUTRON STAR FORMATION	
2.1	Introduction	23
2.2	Ratio a/m of Observed Neutron Stars	26
2.3	Evolution of Ratio a/m after Neutron Star Formation	29
2.4	Ratio a/m of the Core of Main-sequence Stars	35
2.5	Evolution of a/m of Stellar Cores during Post Main-sequence Stage	40
2.6	The a/m Loss during Core Collapse	44
2.7	Discussion and Conclusions	47
Appendix	The Mass Shedding in Relativistic Models	50
	References	52

CHAPTER III GRAVITATIONAL COLLAPSE AND GRAVITATIONAL RADIATION

3.1	Introduction	54
3.2	The Idea of Modelling	57
3.3	A Fast Rotating Non-axisymmetric Model	61
3.4	Implication of the Model	65
3.5	General Consideration on the a/m Change due to Gravitational Radiation	68
	References	71

CHAPTER IV GRAVITATIONAL COLLAPSE AND NEUTRINO PROCESSES

4.1	Introduction	72
4.2	The General Problem of Neutrino Trapping	75
4.3	Gravitational Trapping of Neutrinos	80
4.4	Effects of Gravitational Trapping of Neutrinos in Condensed Objects	85
	References	90

CHAPTER V COLLAPSE OF CHARGED STARS

5.1	Introduction	92
5.2	Collapse of Charged Stars	95
5.3	Motion of Photons in the Reissner-Nordstrom Field	99

5.4	Optical Appearance of a Continuously Collapsing Charged Star	101
5.5	Vibrating Charged Stars	109
5.6	Conclusions	112
	References	114
	MAIN CONCLUSIONS	115
	ACKNOWLEDGEMENT	118
	TABLES AND FIGURES	119

CHAPTER I A SHORT REVIEW OF THE PROBLEM OF

GRAVITATIONAL COLLAPSE AND FINAL STATES

1.1 Introduction

It is well known that at the late stage of the evolution of massive stars, a core made of exhausted materials is formed in its centre. The static equilibrium in the core is still maintained due to the balance of the pressure gradient of degenerated electron gas with gravitational force. Since the silicon shell around the core is still burning, the core material is accreting. Once the mass of the core exceeds the limit which can be sustained by degenerated electron gas, the core collapses under the effect of its own gravity. The result of the stellar core collapse, as it is generally believed, should be the formation of neutron stars, black holes and perhaps naked singularities.

We are interested in the study of the various final states from the point of view of collapsing processes. For example, one of the basic questions in our mind is what will be, after collapsing, the fate of a stellar core initially having a specific angular momentum a larger than its mass m (both a and m are given in the $c=G=1$ unit system). If its angular momentum is lost, we want to know what its

mechanism is and if the angular momentum is conserved, we want to know what configuration the collapse will lead to as the concept of the naked singularity contains several ambiguities. As everybody recognizes, the final answer to this basic question will not be given in the near future. The purpose of the works contained in this thesis, in fact, is intended to prepare the way for a full understanding of these problems.

The thesis contains five chapters. Chapter II is devoted to the a/m issue of the formation of rotating neutron stars. We analyse the main mechanisms for a/m loss during the whole evolution period basing on observational data and existing theoretical models and find out that the existence of a collapsed object with $a > m$ seems to be plausible. Chapter III is devoted to the analysis of gravitational radiation during gravitational collapse. The angular momentum loss due to gravitational radiation is one of key points for the a/m issue analysed in the Chapter II, but it has not yet been well studied. Due to this reason, a fast rotating ellipsoidal model is being worked out with the purpose to have an estimation. And also, some insight about a/m loss in more general situations are given. Chapter IV is devoted to neutrino processes, since they are considered as the most important

physical processes during gravitational collapse. On this subject, our own work concerns the neutrino trapping effect by the strong gravitational field in dense objects. Finally, the Chapter V is dedicated to the study of the optical appearance of collapsing charged stars. As it is well known, collapsing charged objects present properties which resemble those of collapsing rotating objects; in fact, if it is mildly charged, an event horizon will be formed after collapse. And if it is overcharged, the event horizon cannot be formed. In the latter case, the real outcome of collapse is again an interesting open question. Although the reality of a significantly charged star is still a matter of investigation, we assume the existence of charged stars and consider the difference of the optical appearances among the uncharged case (the Schwarzschild black hole), the charged case with event horizon (the Reissner-Nordstrom black hole) and the overcharged case without event horizon. We find some related properties which appear to be very interesting.

In this Chapter I, a short review is given about the relevant topics of the problem which we are concerned. It is devised into three sections according to phases of evolution. The phase before collapse, i.e. the evolution of a massive star at its main-sequence

and post main-sequence stages is in Section 1.2. The phase of collapsing is in Section 1.3. Finally, the phase after collapse, i.e. various final states is contained in Section 1.4.

1.2 The Evolution of Massive Stars before Collapse

In the consideration of stellar core collapse, with the term massive star, we mean a star with a mass in the range of about $10-100M_{\odot}$. In such a star, the nuclear fuel in its central part can be ignited step by step, always under non-degenerated or not highly degenerated condition, and therefore an exhausted core will finally be formed. While the exhausted core is formed, several shells made of Si, O, Ne, C, He and H are successively surrounding the core and the whole star present an onion-like structure. Table 1.1 represents temperatures, densities and overall timescales of various nuclear burning stages which have been calculated for a $25M_{\odot}$ Population I model star by Weaver et al^{1,2}.

We are interested in the late stage of stellar evolution. During this stage, several processes take place which are relevant to the subsequent collapsing phase and worthy being mentioned here.

When the temperature reaches $5 \cdot 10^8$ K or more (after carbon is ignited), the thermal production of neutrino pair, mainly via e^- and e^+ pair annihilation, become significant. The density of the core in this case is still low ($\rho \leq 10^{10} \text{ g cm}^{-3}$, before collapse), so that the core is transparent to neutrinos. Thus, once a neutrino (or anti-neutrino) is produced, it escapes immediately and carries away the

energy. The amount of energy carried away by neutrinos is so large, that stellar evolution in the late stages is considerably sped up.

On the other hand, when the density reaches 10^8 gcm^{-3} or more (silicon is about to be ignited), the Fermi energy of degenerated electron gas is so high that neutronization of the core, via the process $e^- + (Z, A) \rightarrow (Z-1, A) + \nu_e$, takes place leading to several effects: a) the pressure of degenerated electron gas will be reduced, due to the fact that the high energy electron are being captured by nuclei; b) the neutronization process also leads to a further neutrino production, and thus the energy loss due to neutrinos is increasing; c) after the core is neutronized, the main constituents of the core will be neutron rich nuclei such as ^{48}Ca , ^{66}Ni , ^{50}Ti etc., instead of normal nickel and iron. Finally, due to the high temperature in the exhausted core, photodisintegration of heavy nuclei will take place, spending simultaneously the thermal energy of the core.

As a combined effect of those processes, when the accreting core exceeds some critical limit, the equilibrium is seriously broken. At this moment, the core starts collapsing. This is a general picture of the latest evolution of a stellar core, which should be valid qualitatively both for non-rotating³ and rotating⁴ cases. Of course,

the details must depend on the rotation.

In the collapse of a rotating stellar core, there are still several other aspects of the problem which are quite important. For example, what is the mass of a rotating core before collapse? What is the corresponding angular momentum? How is the deformation of the core? And so on. As mentioned above, the basic reason for the collapse is that the gravity of the core cannot be sustained by degenerated electron gas. So to speak, the mass of a collapsing core should be nearly equal to Chandrasekhar mass⁵ which is about $1.4M_{\odot}$ for the non-rotating case. Both model calculations and observed masses of neutron stars are supporting this argument. Weaver et al.¹ calculated that the mass of a non-rotating pre-collapsing core of a $15M_{\odot}$ model star is $1.56M_{\odot}$ and that of a $25M_{\odot}$ model star is $1.61M_{\odot}$. The mass of a collapsing core seems not to depend prominently on the mass of the whole star. In few cases, anyhow, the mass of the neutron star has been actually measured. For example, the masses of components of the binary pulsar 1913+16 as reported by Taylor et al.⁶ to be 1.39 ± 0.15 and $1.44 \pm 0.15M_{\odot}$ are in good agreement with this viewpoint. This argument is wholly true would imply that the mass of a pre-collapsing core depends on its angular momentum, since the Chandrasekhar mass does depend on

the rotation (see for example, Tassoul's book⁷). Ostriker et al.⁸ calculated rapidly rotating white dwarf models by the method of the self consistent field and produced a model having a mass as high as $4.1M_{\odot}$ (the angular momentum of this model is $1.21 \cdot 10^{51}$ ergsec). Then, an interesting question arises: is it possible to have a collapsing core with a mass larger than the limiting mass of a neutron star? This would be very important to know for the understanding of the black hole formation rate. On the angular momentum and deformation of a final configuration before collapse, we have not, till now, any reliable information. However, this is one of our motivation to present an analysis on the angular momentum evolution of stellar cores in Chapter II. When we consider the gravitational radiation in Chapter III, the problem of deformation is concerned again.

1.3 Gravitational Collapse of Stellar Cores

Although it has been definitely argued that core collapse is an inevitable consequence of the evolution of massive stars, the realistic collapse process is still far from being well understood. The difficulties of the problem partially come from the fact that the dynamics of collapse must be fully relativistic and that the time-scale of collapse is very short (of the order of seconds), and partially come from the fact that the physics of very high density and temperature, under which the collapse proceeds, is not clear enough. The complexity of the problem forced people to adopt highly simplified assumptions.

The pioneering work on the collapse was done by Oppenheimer and Snyder⁹ in 1939. They considered a model in which the collapsing object is assumed to be always spherical and pressureless, so it can be thought as the collapse of a spherical dust ball. Of course, there would not be any final equilibrium state for their models (at that time, the limiting mass of a neutron star was known as $0.7M_{\odot}$ ¹⁰, and this might be the reason why they adopted these assumptions). However, the following two important points about the black hole formation were clarified by their pioneering work. First, from the

viewpoint of a distant observer, the collapsing object tends asymptotically towards the gravitational radius, but the observer cannot always see the collapsing object because its luminosity tends to zero asymptotically too as the redshift tends to infinity. Second, the real collapsing process does not end at the gravitational radius. From the viewpoint of a comoving observer, it takes a finite time to cross the gravitational radius; the collapse will then continue to the singularity at $r=0$. The surface at $r=2GM/c^2$ is not a singularity.

These results are fundamentally important, but the further consideration on how they depend on the previously mentioned assumptions (spherical and pressureless) is even more important. In 1966, May and White¹² worked out a spherical collapse model with internal pressure. One of their results proved that the validity of the classical conclusion obtained by Oppenheimer and Snyder does not depend on the assumption of pressureless. Then, to what extent is this picture representative of collapses which are not spherically symmetric? Small perturbations of spherical collapse have been studied in some details^{12,13}. It was shown, specially by Price's work¹³, that if the perturbation is small at the beginning, it remains small when the configuration passes through its event horizon, and so the overall picture is rather

similar to that for spherical collapse. For the highly nonspherical collapse, the situation might be quite different, but the results are not convincing and still far from conclusive. A good review can be found in Miller and Sciama's article.¹⁴

However, the collapse process studied by above mentioned works is too much idealized, in the sense that all physical processes have been ignored and that physical conditions have been oversimplified. During the core collapse, at least, the excessive potential energy must be carried away. It has been found out that the main carrier of the energy is the neutrino¹⁵ which is mainly produced by the inverse β decay of the core matter. Therefore, neutrino processes are crucial for the collapse and should not be ignored in the study of realistic collapse. We will consider it again in Chapter IV.

Another very important problem is the fate of the envelope which was completely ignored by the above mentioned studies. When the core collapses, the envelope temporarily remains stationary. Whenever the core mass is less than the limiting mass of a neutron star, during the collapse, the core bounce will occur nearly at the nuclear density, and a shock wave will propagate outward. Afterwards, a series of question arises. Is the shock strong enough to ignite the matter of

the envelope and induce a supernovae explosion? Will the matter of the envelope be blown away completely, in order to form a neutron star? Or, will the envelope finally fall down and form a black hole? The answer to these questions diverge seriously. Somebody says yes^{1,2} and somebody says no⁴. The answer sensitively depends on several factors which have not yet been clearly found out, such as neutrino trapping, equation of state (specially at high density and low entropy) and so forth. An excellent review on this subject was given by Arnett¹⁶ at the 9th Texas Symposium in 1979.

One more process which is notable is gravitational radiation. People usually think that collapsing stellar cores are one of main astrophysical sources of gravitational radiation. There is still an objection. It was pointed out by Kazanas and Schramm¹⁷ that since neutrino processes will damp out the deformation, gravitational radiation might not be so strong as expected. This problem is left open. However, to the rotation issue of collapse, the gravitational radiation is probably more relevant than the neutrino process. We will consider the effect of gravitational radiation in Chapter III.

1.4 Final States after Collapse

Since final states after collapse can be studied from the static viewpoint as well, we can know them in some details, despite the lack of knowledge about realistic collapse. Final states after collapse are broadly divided into two categories. One is in equilibrium and another one is in non-equilibrium. We first consider final states which are in equilibrium.

As it is known, stellar cores start collapse at a density which is roughly equal to 10^9 gcm^{-3} . At even high densities, the possibility of a stable state which mainly consists of a degenerated neutron fluid was first suggested by Landau¹⁸ in 1932. Baade and Zwicky¹⁹ also suggested the idea of a neutron star independently in 1934. The first quantitative model of a neutron star was built by Oppenheimer and Volkoff¹⁰ in 1939. They found the limiting mass of a neutron star to be $0.7M_{\odot}$, which is notably smaller than the Chandrasekhar mass, due to the fact that they used an oversimplified equation of state of the free degenerated neutron gas. They neglected, however, the effect of nuclear force, specially the repulsive core of nuclear force, despite the fact that the central density has already reached 10^{15} gcm^{-3} , which is even greater than the nuclear density. The discovery of

pulsars²⁰ in 1967 and their identification²¹ as rotating neutron stars in 1968 aroused a great enthusiasm in the study of the neutron star, both in regard of its structure and of its mechanisms of radiation. The problem of studying the neutron star structure lies in the equation of state^{22, 23}. In a typical neutron star model, the density varies from the surface ($\rho_s \approx 10 \text{ g cm}^{-3}$) to the centre ($\rho_c \approx 10^{15} - 10^{16} \text{ g cm}^{-3}$) by 14 to 15 orders of magnitude, but most of the matter is at a density comparable to the central density ρ_c , which is in the supernuclear density range. The equation of state is believed to be reasonably well understood only up to subnuclear density ($\rho < 10^{14} \text{ g cm}^{-3}$) as the low energy nuclear force has been known well enough phenomenologically. For $10^{14} < \rho < 10^{15} \text{ g cm}^{-3}$, the nucleon-nucleon interaction is imperfectly known and the uncertainties on the equation of state mainly arise from the possible neutron and proton superfluid states²⁴ and pion condensation²⁵. For $\rho > 10^{15} \text{ g cm}^{-3}$, the composition is expected to include a significant amount of hyperons. At present, little is known with certainty about the equation of state in this range. Due to uncertainties of the equation of state, resulting neutron star parameters vary considerably. The limiting mass of a neutron star varies by nearly a factor of 5, from $0.6 M_\odot$ to $2.7 M_\odot$ ²². Roughly speaking,

the lower the density at which repulsive nuclear force becomes important and the stronger this force is, the larger is the limiting mass of a neutron star. The central densities of neutron star models vary in the range $2 \cdot 10^{15} - 10^{16} \text{ g cm}^{-3}$ and radii vary from $6 \cdot 10^5$ to $1.3 \cdot 10^6 \text{ cm}$ ²². The value of limiting mass is crucial in the study of the formation rate of neutron stars and black holes, unfortunately, it has not yet been fixed.

Another interesting question is whether it is possible to have new stable configurations with a central density $\rho_c > 10^{16} \text{ g cm}^{-3}$, due to the unknown elementary particle interactions. It seems conceivable, but rather unlikely, as pointed out by Thorne²². The reason is that at these very high densities, the adiabatic index required for the stability against radial perturbation probably exceeds 2.0 and this would violate causality as the speed of sound would then exceed the speed of light. Therefore, the neutron star may be the only stable configuration as final state after collapse.

Then, let us turn to the case in which the mass of a collapsed object is larger than the critical mass and of course, no stable configuration can exist. In this case, under the assumption of spherical symmetry, two conclusions are fundamental. First, although

the collapse constantly develops, after passing through the gravitational radius, the collapsing object cannot have any connection with the outer region and only leaves an event horizon which does not change with time. Second, its gravitational field is always described by the Schwarzschild metric and does not change with time too (it is called Birkhoff theorem²⁶). Such a collapsing object is called a Schwarzschild black hole, which can still be considered as a stationary object.

Before and after 1970, an intensive study was carried on the black hole physics and several important results have been achieved. The following conclusions were mainly obtained by Hawking^{27, 28}, Isreal^{29, 30}, Carter³¹ and Robinson³². a) All stationary black holes (i.e. when settled down into "final" state) are axially symmetric. b) Their characters are uniquely described by three parameters, mass m , charge Q and angular momentum J . This is sometimes called no hair theorem. c) The Kerr-Newman metric³³ is the unique family of solutions which describes the black hole. Thus, the parameters must satisfy a constraint

$$(1.1) \quad m^2 \geq a^2 + Q^2$$

where a is the specific angular momentum and here and hereafter all quantities are expressed in the $c=G=1$ unit system, if numerical value

is not concerned.

Futhermore, several fundamental laws, which must be obeyed by black hole processes, have been found³⁴. The first law of black hole dynamics simply says that energy, momentum, angular momentum and charge are conserved for any black hole process. The specially interesting one is the second law, which says that the area of the black hole horizon can never be reduced by any black hole process; the area A is defined as

$$(1.2) \quad A = 4\pi (m + \sqrt{m^2 - Q^2 - J^2})^2 + a^2$$

This second law, like that of thermodynamics, shows that dynamical processes of black holes are generally irreversible^{35, 36}. An interesting result then follows. Formula (1.2) can be rewritten as

$$(1.3) \quad m^2 = \left(m_{ir} + \frac{Q^2}{4m_{ir}} \right)^2 + \frac{J^2}{4m_{ir}^2}$$

where $m_{ir} \equiv \left(\frac{A}{16\pi} \right)^{1/2}$ is called the irreducible mass of a black hole. From formula (1.3) we see, if we extract Q and/or J from a black hole by a reversible process, by which we mean m_{ir} is conserved, the mass of the black hole is extracted too. However, there is a limit for the reduction of mass. When Q and J have been reduced to zero (i.e. a rotating and charged black hole has been reduced to a Schwarzschild

black hole), m has been reduced to m_{ir} and it can never be reduced anymore, as far as only macroscopic processes are concerned. In this sense, the Schwarzschild black hole can be considered as the ground state of black holes.

Then, we turn to the cases in which formula (1.1) is disobeyed and an event horizon cannot be formed. The first question in this case, is what the final state will be. On this matter, there is a considerable amount of uncertainty due to the fact that one possible outcome has been envisaged as a naked singularity, but such an object would break down physical laws in the region nearby it. Moreover, it has been shown recently by Clarke and de Felice³⁷ that timelike naked singularities, which are described by some exact solutions of Einstein equations, imply global causal violation. Under this circumstance, different attitudes of mind have been presented. Some people think the naked singularity should not exist. Penrose³⁸ in fact asks: "does there exist a cosmic censor who forbids the appearance of naked singularity clothing each one in an absolute event horizon?" This is known as the hypothesis of cosmic censorship. Some people, on the other hand, still think the so-called naked singularity can exist in nature as well.

By assuming the existence of naked singularities, some suspicious but interesting connection between the naked singularity and black hole is reached. a) The Kerr-Newman naked singularity is unstable, in the sense that the Kerr-Newman naked singularity can lose its angular momentum and/or its charge and so to transform into a black hole, but the opposite is impossible. The non-rotating, charged case was proved by Cohen et al.³⁹ and the uncharged rotating case was proved by de Felice⁴⁰. b) The optical appearance of stellar collapse in the formation of naked singularity is the same as that in the formation of black hole. The uncharged rotating case has been discussed by de Felice⁴¹ and the charged, non-rotating case is discussed in Chapter V of this thesis.

References for Chapter I

- 1) T.A.Weaver, G.B.Zimmerman and S.E.Woosley; (1978) Ap J 225, 1021.
- 2) T.A.Weaver and S.E.Woosley; (1980) Ann N Y Acad Sci 336, 335.
- 3) W.D.Arnett; (1977) Ap J Suppl 35, 145.
- 4) E.Müller and W.Hillebrandt; (1981) Astron Astrophys 103, 358.
- 5) S.Chandrasekhar; (1931) Monthly Notice R A S 91, 456.
- 6) J.H.Taylor and P M McCulloch; (1980) Ann N Y Acad Sci 336, 442.
- 7) J.L.Tassoul; (1978) Theory of Rotating Stars Ch 13 Prin Univ Press.
- 8) J.P.Ostriker and P.Bödenheimer; (1968) Ap J 151, 1089.
- 9) J.R.Oppenheimer and H.Snyder; (1939) Phys Rev 56, 455.
- 10) J.R.Oppenheimer and G.M.Volkoff; (1939) Phys Rev 55, 374.
- 11) M.M.May and R.H.White; (1966) Phys Rev 141, 1232.
- 12) V.de la Cruz, J.E.Chase and W.Isreal; (1970) Phys Rev Lett 24, 423.
- 13) R.H.Price; (1972) Phys Rev D5, 2419 and D5, 2439.
- 14) J.C.Miller and D.W.Sciama; (1980) General Relativity and Gravitation,
Vol II, Ch 9, Ed A Held, Plenum Press, New York and London.
- 15) S.Shapiro; (1979) Sources of Gravitational Radiation, Ed L L Smarr,
p 355, Cambridge Univ Press.
- 16) W.D.Arnett; (1980) Ann N Y Acad Sci 336, 366.
- 17) D.Kazanas and D.N.Schramm; (1977) Ap J 214, 819.

- 18) L.Landau; (1932) Physik Zeits Soviet Union 1, 285.
- 19) W.Baade and F.Zwicky; (1934) Phys Rev 45, 138.
- 20) A.Hewish, S.J.Bell, J.D.H.Pilkington, P.F.Scott and R.A.Collins; (1968)
Nature Lond 217, 709.
- 21) T.Gold; (1968) Nature Lond 218, 731.
- 22) K.S.Thorne; (1966) Proc Int School of Phys Enrico Fermi 35, 166.
- 23) W.D.Arnett and R.L.Bowers; (1977) Ap J Suppl 33, 415.
- 24) N.C.Chao, J.W.Clark and C.M.Yang; (1972) Nucl Phys A179, 320.
- 25) J.B.Hartle, R.F.Sawyer and D.J.Scalapino; (1975) Ap J 199, 471.
- 26) G.D.Birkhoff; (1923) Relativity and Modern Physics, Havard Univ Press.
- 27) S.Hawking; (1971) Phys Rev Lett 26, 1344.
- 28) S.Hawking; (1972) Commun Math Phys 25, 152.
- 29) W.Isreal; (1967) Phys Rev 164, 1776.
- 30) W.Isreal; (1968) Commun Math Phys 8, 245.
- 31) B.Carter; (1970) Phys Rev Lett 26, 331.
- 32)
- 33) C.W.Misner, K.S.Thorne and J.A.Wheeler; (1973) Gravitation P 877
W H Freeman and Co.
- 34) J.M.Bardeen, B.Carter and S.Hawking; (1973) Commun Math Phys 31, 161.
- 35) D.Christodolou; (1970) Phys Rev Lett 25, 1596.

- 36) D.Christodolou and R.Ruffini; (1971) Phys Rev D4, 3552.
- 37) C.Clarke and F.de Felice; (1982) J Phys A 15, 2415.
- 38) R.Penrose; (1969) Nuo Cim Special Number 1, 252.
- 39) J.M.Cohen and R.Gautreau; (1979) Phys Rev D19, 1273.
- 40) F.de Felice; (1978) Nature Lond 273, 429.
- 41) F.de Felice, M.Calvani and L.Nobili; (1978) Nuo Cim Lett 23, 539.

CHAPTER II STELLAR ROTATION AND NEUTRON STAR FORMATION[†]

2.1 Introduction

As mentioned in Chapter I, a collapsing rotating and uncharged object with specific angular momentum a larger than its mass m will not be covered by an event horizon and what it will be is an open question. Therefore, it would be interesting to find out whether there is some evidence about the existence of such a rapidly rotating collapsing object.

Unfortunately, till now no direct observational evidence about the rotation of black holes is available, so we are forced to focus our attention to neutron stars; they are in fact, collapsed objects with a mass not too much lower than that of the limiting mass of a black hole. Moreover, we have good observational materials about the rotation of neutron stars, that we gather from their pulsating periods.

[†] The main part of the work contained in this chapter has been published in the JOURNAL OF PHYSICS A, VOL. 15, P.3341 (1982), jointly with F. de Felice, under the title STELLAR ROTATION AND GRAVITATIONAL COLLAPSE: THE a/m ISSUE.

Usually, neutron stars are thought to be fast rotators, while normal stars are thought to be slow rotators, since the former have a period of the order of seconds and the latter have a period of the order of days. From the viewpoint of evolution, this idea is somehow misleading. If we characterize the stellar rotation by its specific angular momentum, we reach the opposite conclusion that neutron stars are slow rotators and normal stars are fast rotators. Thus, in the course of evolution, we should find physical mechanisms which cause a LOSS of the specific angular momentum. This is going to be the subject of the present chapter.

In studying the final state of a collapsing rotating object, the dimensionless ratio a/m is a suitable parameter and it is used through this and the next chapter. We consider the $a/m \ll 1$ case as that of a slow rotator, the $a/m \approx 1$ case as that of a fast one and the $a/m \gg 1$ case as that of a very fast one. Later on we shall see that the cores of main-sequence stars are very fast rotators having ratio a/m as high as $10-10^2$ (in Section 2.4), while observed neutron stars are slow rotators having ratio a/m as low as $10^{-2}-10^{-3}$ (in Section 2.2). This huge gap seems to suggest that during evolution, the ratio a/m is strongly depressed. Therefore, black holes would probably be slow

rotators and fast rotating collapsed objects such as naked singularities are out of reality. Our analysis will show that this statement is probably not true. For the formation of a neutron star, we find that some strong reduction occurs after collapse has stopped, implying that the existence of a rapidly rotating collapsed object is actually possible.

In the following analysis, the evolution of the ratio a/m is divided into three stages. The evolution in the post main-sequence stage is considered in Section 2.5. Loss of ratio a/m during the collapse is discussed in Section 2.6. After a neutron star has been formed, some mechanisms dissipating its rotational energy and reducing the ratio a/m are analysed in Section 2.3. The final discussion and conclusions are presented in Section 2.7.

2.2 Ratio a/m of Observed Neutron Stars

only a few months after pulsars were discovered by Hewish et al.¹, Gold² recognized that they are rotating neutron stars. Therefore, rotational periods of neutron stars can be accurately measured by means of radio techniques. As mentioned in 1.4, observed periods of neutron stars are of the order of seconds which are shorter than those of normal stars by about five orders of magnitude. Since the density of a neutron star is very high and the moment of inertia is small, its angular momentum is not necessarily large. In this section, we shall determine the ratio a/m of neutron stars using observational data and theoretical models, and shall show that their ratio a/m are in fact very small.

Beside the period ω which has been known by observation, we still have to know the mass M and the moment of inertia I , in order to calculate the ratio a/m , since by definition,

$$(2.1) \quad \frac{a}{m} \equiv \frac{Jc}{GM^2} = \frac{Ic}{GM^2} \omega$$

where J is the angular momentum, G is the gravitational constant and c is the speed of light. The masses of neutron stars, as pointed out in 1.4, have been measured only in a few cases and have the value of about $1.4M_{\odot}$. From theoretical considerations, we know that masses

of neutron stars should not be widely varied. Because of this reason, we shall assume the mass of any neutron star as $M=1M_{\odot}$. About the moment of inertia, surely, we do not have any observational evidence.

Let us make a simple estimation, assuming an average density $\bar{\rho}=5 \cdot 10^{14} \text{ g cm}^{-3}$ and a radius $R=10^6 \text{ cm}$, We get

$$(2.2) \quad I = \frac{8\pi}{15} \rho R^5 = 10^{45} \text{ g cm}^2$$

Arnett et al.³ calculated moments of inertia of neutron star models by using 10 different equations of state and got values in the range $6 \cdot 10^{44} - 2 \cdot 10^{45} \text{ g cm}^2$. It proves that (2.2) is a fairly good estimation.

Substituting these values into (2.1), we have a formula for evaluating the ratio a/m of neutron stars

$$(2.3) \quad \frac{a}{m} = 0.57 \cdot 10^{-3} P^{-1} (\text{sec})$$

where P is the rotational period.

In Table 2.1, observational data of periods for 105 samples, which are taken from Smith's⁴ book "Pulsars", have been listed and the corresponding ratio a/m have been calculated by (2.3). From these 105 samples, we find that the ratios a/m are distributed as follows:

$a/m > 10^{-2}$	1 sample (Crab pulsar, 0531+21)
$10^{-2} > a/m > 5 \cdot 10^{-3}$	1 sample (Vela pulsar, 0835-45)
$5 \cdot 10^{-3} > a/m > 1 \cdot 10^{-3}$	44 samples

$1 \cdot 10^{-3} > a/m > 5 \cdot 10^{-4}$ 33 samples

$5 \cdot 10^{-4} > a/m > 1 \cdot 10^{-4}$ 26 samples.

For most samples of this ensemble (98%), the ratio a/m does not vary widely. It ranges in a rather narrow interval, from $3.6 \cdot 10^{-3}$ to $1.5 \cdot 10^{-4}$.

Crab pulsar (0531+21) is a special member and of special importance

being the youngest one (age $T=928$ yrs). It has the longest period

($P=33$ ms, $a/m=1.7 \cdot 10^{-2}$) and the largest changing rate of the period

($\dot{P}=36.5$ ns/d). From Table 2.1 and above considerations, we shall simply

assume that the ratio a/m of observed neutron stars is nearly equal

to or much less than 10^{-2} .

2.3 Evolution of Ratio a/m after Neutron Star Formation

Since the pulsating radiation of a neutron star originates from the rapid rotation of its magnetic configuration, the radiation should carry away rotational energy. As Predicted by Gold² in his first paper a slight but steady slowing down of observed frequencies was really found first in the Crab pulsar⁵, then in the others⁶. The importance for us of this fact is that the ratio a/m of a neutron star at the very beginning of its formation should be larger than that at a subsequent time. Then, an interesting point is to know how fast it rotated at the beginning.

Before considering this point, let us first calculate, with a simple Newtonian argument, the limiting value of ratio a/m which can be sustained by a neutron star. In the limiting case, we suppose that the centrifugal force at the equator is just balanced by the gravitational force before mass shedding takes place. Assuming again the neutron star as a rigidly rotating uniform sphere, we have the following relation for the critical angular velocity ω_{crit} .

$$(2.4) \quad \omega_{crit}^2 = \frac{GM}{R^3}$$

Using the definition $a/m = I\omega c/GM$, the critical value of a/m is obtained.

$$(2.5) \quad \left(\frac{a}{m}\right)_{\text{crit}} = 1.03 \left(\frac{M}{M_0}\right)^{-1/2}$$

where the representative value of $\bar{\rho} = 5 \cdot 10^{14} \text{ gm}^{-3}$ has been used. Formula (2.5) tells us that the maximum value of a/m that can be sustained by a neutron star is about one[†]. The observed values of ratio a/m are all

† Since in the critical case the star should be seriously deformed, this argument seems quite doubtful. In this note, however, we would like to show that formula (2.5) does mean something related to mass shedding.

Instead of a rigidly rotating uniform sphere we should consider it as a rigidly rotating uniform spheroid, i.e. a Maclaurin spheroid (see e.g. Tassoul's book⁶). By formulas (48)-(54) and figures (4.1) and (4.2) of Chapter 4 of Tassoul's book, we find that the critical case defined by (2.5) corresponds to $e=0.95$ or $b/a=0.3$. It is in fact seriously deformed. If we consider the rotation parameter τ which is defined as the ratio of rotational energy to potential energy, the value τ of this critical case is calculated to be 0.27. It is just the limit for secular instability of Maclaurin spheroid (see P.240 in the above cited book). Therefore we have reason to say that if it rotates faster than the critical case, mass shedding will take place.

The critical value of a/m calculated from relativistic models is presented in the Appendix. (30)

much smaller than one, so they are stable enough. Then, we are interested to know what was the situation at the beginning.

It is definitely known that the pulsating radiation is decreasing the rotational energy of a neutron star. Let us now consider this effect first. Assuming that the pulsating radiation is the unique effect in dissipating rotational energy and that it can be considered as the magnetic dipole radiation, we have

$$(2.6) \quad \frac{d(\frac{1}{2}I\omega^2)}{dt} = -L = -K\omega^4$$

where L is the luminosity and K is proportional to the square of magnetic dipole moment. Formula (2.6) can be rewritten as

$$(2.7) \quad \frac{d\omega}{dt} = \frac{-K}{I} \omega^3$$

since the moment of inertia I is almost a constant. Moreover, if we assume that the magnetic dipole moment is a constant, (2.7) can be solved as

$$(2.8) \quad T = \frac{I}{K} \left(\frac{1}{\omega^2} - \frac{1}{\omega_0^2} \right)$$

where T is the age of a neutron star and ω_0 is the initial angular velocity which we are interested in. Using (2.7) and changing ω to period P , we have

$$(2.9) \quad T = \frac{P}{2\dot{P}} \left(1 - \frac{P_0^2}{P^2} \right)$$

where P_0 is the initial period. Suppose P_0 is much smaller than P ,

thus the age T would be equal to $P/2\dot{P}$. Values of $P/2\dot{P}$ for various pulsars have been listed in Table 2.1. Only for the Crab pulsar, we know its age exactly, which is 928yrs. Its true age is significantly shorter than the presumed age $P/2\dot{P}$ implies that P_0 is not too much shorter than P . In fact, formula (2.9) tells $P_0 \approx P/2$. For the other pulsars, the argument is not so clear, but usually people think the presumed age $P/2\dot{P}$ would be larger than the true age due to the decay of magnetic moment. Since the decay timescale has been estimated as to be 10^6 yrs⁴, this argument holds for most samples of our ensemble (66 out of 82) which have an "age" larger than 10^6 yrs. For the youngest Crab pulsar with an age of 10^3 yrs, the decaying effect of magnetic moment should not be prominent. Therefore, we conclude that if the pulsating radiation is the unique mechanism for slowing down the rotation, initial neutron stars would remain slow rotators having the ratio a/m much less than 1.

Are there other mechanisms which also slow down the rotation? By noting two facts that neutron stars have large proper velocities and the magnetic configuration of a star is usually deviated from its geometric centre, Harrison and Tademaru⁷ suggested an off-centered dipole model for neutron stars. The radiation of a rotating

off-centered dipole induces not only a torque but also a net force due to the asymmetry of radiation and this force would accelerate neutron stars. By this model, both radiative energy and translational kinetic energy come from the rotational energy. Let us consider, in this case, what the initial a/m of a neutron star would be.

The equations of motion derived by Harrison and Tademaru are

$$(2.10) \quad \frac{d}{dt} (Mv) = \frac{L}{c} \left(\epsilon - \frac{v}{c} \right)$$

$$\frac{d}{dt} (I\omega) = - \frac{L}{\omega} \left(1 + \frac{\epsilon v}{c} \right)$$

where ϵ is called the radiation asymmetry coefficient, which depends on the separation of the magnetic dipole from the spin axis, and also on other factors. Since $\frac{\epsilon v}{c} \ll 1$, equations (2.10) reduce to

$$(2.11) \quad M \frac{dv}{dt} = - \frac{\epsilon}{c} \frac{d}{dt} \left(\frac{1}{2} I \omega^2 \right)$$

and from this equation, it follows that

$$(2.12) \quad Mv = \frac{\langle \epsilon \rangle}{2c} I (\omega_0^2 - \omega^2)$$

where $\langle \epsilon \rangle$ is an averaged asymmetry coefficient. Formula (2.12) gives the relation among the observed translational velocity, observed angular velocity and initial angular velocity and that is just what we need.

Unfortunately, we cannot evaluate the asymmetry coefficient ϵ due

to the lack of detailed knowledge of the magnetic configuration. However, a semi-quantitative conclusion is ready. The translational velocity V of a pulsar has been evaluated to be larger than 100 km s^{-1} for most cases ^{8, 9, 10}. A detailed analysis of the selection effects on the scintillation observations of pulsar radiation leads to a most probable lower limit for pulsar velocities of 120 km s^{-1} ^{11, 12}. In fact, MV is much larger than $\frac{1}{2} \frac{\omega^2}{c}$, even for extreme cases. Then, formula (2.12) tells that ω_0 is much larger than ω . This is just the interesting point from our point of view, because it means that a large amount of a/m is reduced after the neutron star has formed. Quantitatively, assuming a mild value of 10^{-2} for ϵ , we find that the initial angular velocity ω_0 reaches 10^4 s^{-1} , thus the initial value of ratio a/m reaches about one, which is just the critical limit as shown by formula (2.5). Therefore, the existence of a collapsed object as a fast rotator with $a/m \approx 1$ is indeed possible, if the Harrison and Tademaru mechanism holds true. Surely, in order to make this argument to be convincing, some other evidences are needed.

2.4 Ratio a/m of the Core of Main-sequence Stars

Now we turn our attention to the beginning of stellar evolution, in order to know what the value of ratio a/m of main-sequence stellar cores are. Afterwards, we will try to track its evolution, hoping to see from another angle, what the resulting value of a/m after core collapse will be.

The projected rotational velocity $V_e \sin i$ of normal stars can be evaluated from the overall spectral broadening, where V_e is the rotational velocity at the equator and i is the angle between the rotational axis and line of sight. Can we know V_e itself? It was demonstrated by Chandrasekhar and Munch¹³ that, if we have a representative sample of stars belonging to one spectral type, and if the axes of rotation are distributed at random in space, we have

$$(2.13) \quad \langle V_e \rangle = \frac{4}{\pi} \langle V_e \sin i \rangle$$

where the bracket used here stands for taking average.

Even if we know the rotational velocity V_e , hence know the angular velocity ω at the equator, it is still a non-trivial problem to calculate the angular momentum of a star and of its stellar core, since it depends on the mass and angular velocity distribution within the star. For the latter in particular, we have no knowledge whatsoever,

neither from theory nor from observation. This situation forces us to adopt simplified assumptions to evaluate the ratio a/m .

For our purpose, the main point is to know the ratio a/m of the core of main-sequence stars. Before doing that, it is interesting to get an idea about what the value of a/m of a whole star is. As an order of magnitude, the ratio a/m of main-sequence stars with $M \leq 10M_{\odot}$ has been estimated assuming it as a rigidly rotating uniform sphere, thus

$$(2.14) \quad \frac{a}{m} = \frac{2 R V_e c}{5 G M}$$

R as the radius is calculated from $(\frac{L}{4\pi\sigma T^4})^{1/2}$, where L is the luminosity, T is the effective temperature and σ is Stefan-Boltzmann constant, the relevant data being taken from Tinsley¹⁴. V_e is obtained from (2.13) with data deduced by several authors^{15,16}. Results are listed in Table 2.2. From the table we see, ratio a/m of early type stars (B, A and early F types) are of the order of 10^2 .

This result is supported by another observational evidence. The mass shedding for B_e stars shows that their equatorial velocity should have reached the critical limit of stability. From the theoretical consideration, the parameter τ (defined as the ratio of rotational energy and gravitational energy) for mass shedding ranges between

0.14 and 0.25¹⁷. In our models, the relation of a/m and τ simply reads

$$(2.15) \quad \frac{a}{m} = \frac{1.2c}{V_e} \tau$$

Therefore, for an observed rotational velocity for B_e stars of 400 km s^{-1} ,¹⁸ the ratio a/m ranges between 120 and 220. It is consistent with above estimations. This result proves that a normal star is in fact a very fast rotator, comparing to a neutron star.

From now on, we concentrate to the stellar core which will finally evolve to a neutron star. Since we do not know the internal distribution of angular velocity, we consider two presumed cases.

Case A. Rigid rotation

Let us consider a $1M_\odot$ core of a main-sequence star with following parameters

$$(2.16) \quad M = 10 M_\odot, \quad R = 3.3 \times 10^{11} \text{ cm}, \quad V_e = (2-4) \cdot 10^7 \text{ cm s}^{-1}$$

and

$$\omega = \frac{V_e}{R} = (0.6-1.2) \cdot 10^{-4} \text{ s}^{-1}$$

Under the assumption of rigid rotation, the angular velocity of core is the same as shown by (2.16). Besides, we still have to assume the density distribution. Since the core is rather small, the density of core can be considered as uniform, then we have the expression of a/m

$$(2.17) \quad \frac{a}{m} = \frac{2c}{5GM} R^2 \omega = 5.5 \cdot 10^5 \left(\frac{M}{M_\odot} \right)^{-\frac{1}{2}} \bar{\rho}^{-\frac{2}{3}} \omega$$

About the value of density, we have known that the average density $\bar{\rho}$

of whole star is 0.15gcm^{-3} and the central density ρ_c is about 7.8gcm^{-3} .¹⁹

Taking several representative core densities, corresponding values of a/m of cores are shown in Table 2.3. It suggests that the most plausible estimation of ratio a/m of a $1M_\odot$ core, with the assumption of rigid rotation, is in the range of $a/m=(10-50)$.

Case B. Differential rotation

If convective motions are important in the stellar interior, then it is likely that the angular momentum is redistributed so that differential rotation sets up. Since the angular momentum distribution in the rotating star is completely unknown, Bodenheimer²⁰ built several rotating main-sequence stellar models by assigning various angular momentum distribution laws. Let us pick up some data from his models and evaluated the ratio a/m of corresponding $1M_\odot$ cores. Quantitatively, in all these cases, the stellar core has more angular momentum than it would have in the corresponding rigid rotating case. Therefore, the resulting value of a/m is always larger.

In Table 2.4, five models are listed for our purpose, in the last line of the table, a/m is evaluated from formula (2.17), assuming that the core has a uniform density $\rho = \rho_c$ and a uniform angular velocity $\omega = \omega_c$, where ρ_c and ω_c are respectively the central density and

central angular velocity of the corresponding model.

Model I is a rigid rotating $15M_{\odot}$ star with a similar V_e as considered in Case A. The resulting a/m is also similar. Model II describes a differentially rotating star with the same J and M as in Model I; the ratio a/m is therefore larger and the resulting V_e is smaller. Since V_e of Model II seems too small compared with typical observed values, we choose another $15M_{\odot}$ model with the same angular momentum distribution law as that of Model II, but with a larger J . That is Model III. Correspondingly, the ratio a/m is about 10^2 which is larger than the value estimated in Case A. Model IV and V describe a $30M_{\odot}$ star with two different angular momentum distribution laws and reasonable values of V_e . In both cases, Ratios a/m are of the same order of 10^2 .

Combining cases A and B, we can conclude that the ratio a/m for a $1M_{\odot}$ stellar core of massive rotating main-sequence stars, with V_e equal to $(200-400)\text{kms}^{-1}$, ranges from 10 to 100.

2.5 Evolution of a/m of Stellar Cores during Post Main-sequence

Stage

Although the main-sequence stage is the longest period in the whole life of a star, we don't think the change of a/m of the core is important in this stage, since no prominent structural change happens. Quite on the contrary, the post main-sequence stage is not so long as the main-sequence stage, but the stellar structure changes rapidly. The core shrinking and envelope expanding in the post main-sequence stage must induce an angular momentum transfer from the core to envelope, otherwise, the centrifugal force in the core would exceed the gravitational force making this configuration unstable.

We are interested to know how much angular momentum will be transported out from a core with a fixed mass during post main-sequence stage. Unfortunately, almost all rotating stellar models were designed by assigning an angular momentum distribution law. In these models, the amount of angular momentum loss of the core is somehow arbitrary due to the artificial distribution law. Therefore, it does not suit us. However, Endal and Sofia^{21,22} built some rotating stellar models by considering a more realistic process of angular momentum redistribution. They found that the convection and Eddington circulation

are the most important mechanisms for redistributing the angular momentum in a star. Let us see what information we can get from their computational data.

They evolved a $7M_{\odot}$ stellar model from zero age main-sequence with rigid rotation at a rate of $\omega = 8.8 \cdot 10^{-5} \text{ s}^{-1}$ to the double shell burning period. Their final configuration has a central density $\rho_c = 1.7 \cdot 10^7 \text{ gcm}^{-3}$ and $\omega_{\text{core}} \approx 0.4 \text{ s}^{-1}$ (from their Fig.4, $\log \omega_{\text{core}} \approx -0.4$). Then let us make some estimations. At its main-sequence stage, the core density should be assumed as 10 gcm^{-3} ; then combining with its initial angular velocity the ratio a/m of the core in its main-sequence stage is evaluated from formula (2.17) as to be 10.4. For its final configuration, assuming an average core density $\bar{\rho} = 1 \cdot 10^7 \text{ gcm}^{-3}$, combining with its final core angular velocity, the final value of a/m is estimated, again from formula (2.17), as to be 5. This is to say, half of the initial angular momentum has been carried out of the core.

They have also worked out a $10M_{\odot}$ stellar model and evolved it from zero age main-sequence to carbon ignition, a time span covering about 98% of the time requested to reach the core collapse. By some mechanisms, they found that the effect of angular momentum redistribution is to decrease the angular momentum of the core by 40%. It is almost the

same as the reduction rate which we have estimated for their $7M_{\odot}$ model.

Consequently, we conclude as follows. If the material interchange is in fact the dominant mechanism of angular momentum transfer, and the reduction rate can be estimated as one half, combining with the value of a/m estimated for main-sequence cores in the last section, we suggest that the precollapse core would have a/m in the range 5-50, which is notably larger than 1.

However, the magnetic field effect has not been included in Endal and Sofia's models, then also in above consideration. Although in another paper²³, they argued that it is not important, there are still some reasons to believe that it might be far more effective than the material interchange mechanism. Since the effect of magnetic field to the angular momentum redistribution has not been calculated, the following arguments may be helpful.

Suppose there were no angular momentum transfer in the star during its post main-sequence evolution, a very large gradient of angular velocity would then appear, due to the core shrinking and envelope expanding; and thus the magnetic field lines would be seriously twisted. The magnetic field always tends to force the plasma to move along the field lines. On the other hand, the inertia of the moving

plasma tends to let itself be moved straightforwardly. This tendency will cause field lines to resist being twisted and will maintain a smaller gradient of angular velocity in the star. It serves just as a mechanism of angular momentum transfer from the inner part toward the outer part. The point lies in its efficiency.

The following idea was suggested by Mestel²⁴. At the beginning of the post main-sequence stage, the magnetic linkage between core and envelope can be considered as tight enough to maintain a corotation. While core contraction and envelope expansion continue, more and more field lines gradually detach and the magnetic linkage becomes weaker and weaker. Let us image an effective time T . The rigid corotation is effectively maintained, as if $t < T$; the magnetic linkage can be considered as being broken, at the time $t > T$, thus the angular momentum of the core would be locally conserved. As pointed out by Mestel, a very short time T (compared with the post main-sequence lifetime) is enough to induce a reduction of a/m by one order of magnitude.

This argument seems compelling, but we cannot reach any conclusion before we have a better idea of how long a T can be considered as reasonable. However, it shows that the magnetic effect is possibly important and worthy to be taken into account in building a rotating stellar model.

2.6 The a/m Loss during Core Collapse

Are there any mechanisms for carrying away a large amount of angular momentum during core collapse which proceeds in the dynamical timescale (of the order of seconds)? As mentioned in Chapter I, two candidates are neutrino emission and gravitational radiation.

One of dominant mechanisms of neutrino production during stellar core collapse is the inversed β -decay of nuclei,

$$(2.18) \quad e^+ + (z, A) \longrightarrow (z-1, A) + \nu_e$$

since in this case the Fermi energy of degenerated electron gas is high enough. Despite the weakness of interaction, the production rate can reach as high as $10^{39} \text{ s}^{-1} \text{ cm}^{-3}$ ²⁵, due to the very high density of stellar matter ($\rho \geq 10^{10} \text{ g cm}^{-3}$). It was argued²⁴ that neutrino emission is in fact the dominant mechanism to carry away the excessive energy during the collapse. Then, is it also an efficient mechanism to carry away angular momentum? The answer is no, mainly in consideration of the fact that neutrino emission is isotropic relative to the star. However, it does carry away some angular momentum. Because of the relativistic effect of stellar rotation and collapse, neutrino flow is asymmetric relative to the rotation axis from the viewpoint of a distant observer. Kazanas²⁶ has estimated that about 10% of total

angular momentum of a rotating stellar core is being carried away by neutrino during stellar collapse. At the same time, we must notice that the ratio a/m depends on both J and M , and the mass-energy of stellar core is being carried away simultaneously. The net change rate of a/m reads

$$(2.19) \quad \frac{d\left(\frac{a}{m}\right)}{\left(\frac{a}{m}\right)} = \frac{dJ}{J} - \frac{2dM}{M}$$

If we consider dM as the total excessive potential energy, we find that $\frac{|dM|}{M} \approx 10^{-1}$, thus $\frac{d\left(\frac{a}{m}\right)}{\left(\frac{a}{m}\right)}$ might be even positive. At least, we can safely say, neutrino emission is not an important mechanism for the problem we are studying.

What about gravitational radiation? It is usually thought that this process is also an important one during the collapse and that it may carry away a large amount of angular momentum²³. In the last ten years, a considerable amount of work has been produced on this subject. Since the gravitational wave has not yet been detected, the main attention is devoted to calculate the spectrum and the total energy emitted by those presumed astrophysical sources. Much less attention has been paid to the angular momentum loss due to its ^(importance) minor and greater uncertainty. Since it is one of the key point in our analysis, it motivates us to make a modelling estimation. The favour-

able result is that, if the initial a/m is 5-10, and a large non-axisymmetry is maintained during the collapse, one may expect one order reduction of a/m . The details are shown in the next chapter.

2.7 Discussion and Conclusions

As observational facts, we have pointed out that a $1M_{\odot}$ core of main-sequence stars with a mass in the range $(10-30)M_{\odot}$ and with an equatorial velocity in the range $(200-400)\text{kms}^{-1}$ should have the value of a/m in the range 10-100; the rotating neutron stars, on the other hand, have the value of a/m nearly equal to or much less than 10^{-2} . The question arises therefore of when and how the core reduces its a/m for about four orders of magnitude (see Table 2.5). After surveying the various phases which could be relevant, we summarize conclusions as follows.

a) If we forget all uncertainties involved in the analysis, we can outline the following scenario which is consistent with our analysis in all its aspects (see also Table 2.5). At the beginning, main-sequence stellar cores have a/m in the range 10-20. During its post main-sequence evolution, about half of its angular momentum is transported out mainly due to matter exchange. Therefore, when star reaches its precollapse configuration, the ratio a/m of cores remain within 5-10. During core collapse, gravitational waves are the main carrier of the lost angular momentum, while neutrinos are not relevant. When the collapse has stopped, the ratio a/m of a newly formed neutron star is about 1 (see the next chapter). Because of the asymmetry of

the magnetic configuration of a newly formed neutron star, the radiative reaction force accelerates the star on the expenses of its rotational energy. This effect (called Harrison-Tademaru effect) would reduce the ratio a/m of the neutron star from 1 to 10^{-2} . For a young pulsar (much younger than 10^6 yrs), the pulsating radiation does not dissipate too much energy, so the finally observed value of a/m is still of the order of 10^{-2} . For an old pulsar (nearly equal or larger than 10^6 yrs), the pulsating radiation has spent a significant amount of rotational energy, thus the observed value of a/m is one order less.

b) Whenever the Harrison-Tademaru effect holds true, the collapsed object as a fast rotator with $a/m \approx 1$ is quite plausible. Therefore a reduction of a/m for one or two orders of magnitude is needed in the post main-sequence period and collapse period. Except the ideal case shown in conclusion a), it implies that a realistic stellar model of a post main-sequence star must involve an even stronger mechanism for angular momentum transfer than those elaborated by Endal and Sofia. The possibly important effect from a magnetic field is worthy to be concerned.

c) If the Harrison-Tademaru effect is excluded, a reduction of a/m of three or four orders of magnitude is need in the post main-

sequence period and collapse period. From the analysis presented in this chapter, we cannot see any indication of the presence of such effective mechanisms. This is probably a counterevidence in favour of the Harrison-Tademaru mechanism.

Appendix The Mass Shedding in Relativistic Models

In this appendix, we show that by relativistic model, the maximal value of a/m which can be sustained by a fast rotating object is also about 1. The referring models were worked out by Butterworth and Ipser²⁷ in 1976.

They constructed several sequences of uniformly rotating homogeneous bodies which is in fact the relativistic analogues of the classical Maclaurin spheroids. Each of their sequences has a fixed γ_s which is defined as

$$(2.20) \quad \gamma_s = 1 - \left(1 - \frac{2m}{r_s^*}\right)^{1/2}$$

where r_s^* is the Schwarzschild radial coordinate of the surface of configurations defined as $\left(\frac{3m}{4\pi\epsilon}\right)^{1/3}$. The configuration varied in each sequence is characterized by a rotational parameter $\frac{\Omega^2}{\epsilon}$. Ω is angular velocity and ϵ is density. Both are constants in their models. They found by calculations that when rotational parameter reaches some critical value, mass shedding happens at the equator. It is just the same limiting case in which we are interested.

Our purpose is to compute the critical value of a/m from the data reported in their paper. The conversion formula from their data to a/m is designed as follows.

$$(2.21) \quad \left(\frac{Q}{m}\right)^2 = \left(\frac{I\Omega}{M^2}\right)^2 = \left(\frac{\Omega^2}{\epsilon}\right)(I\epsilon^{3/2})^2 \left(\frac{r_s^*}{2M}\right)^6 \left(\frac{32\pi}{3}\right)^2$$

where $\frac{\Omega^2}{\epsilon}$ and $I\epsilon^{3/2}$ can be taken from their Table 1 to 3, $\frac{r_s^*}{2m}$ can be calculated from (2.20). The results are listed in Table 2.6. It shows that the critical value of a/m is larger than and of the order of 1, and the corresponding relativistic parameter $\frac{r_s^*}{2m}$ is less than 2.

We consider it as another relevant fact in supporting the conclusion that a newly formed neutron star may have the value of a/m of the order of 1.

References for Chapter II

- 1) A Hewish, S J Bell, J D H Pilkington, P F Scott and R A Collins;
(1968) Nature Lond 217, 709.
- 2) T Gold; (1968) Nature Lond 218, 731.
- 3) W D Arnett and R L Bowers (1977) Ap J Suppl 33, 415.
- 4) F G Smith; (1977) Pulsars Cambridge Univ Press Cambridge.
- 5) D W Richards and J M Comella; (1969) Nature Lond 222, 551.
- 6) J L Tassoul; (1978) Theory of Rotating Stars Princeton Univ Press
Princeton.
- 7) E R Harrison and E Tademaru; (1975) Ap J 201, 447.
- 8) V Trimble; (1971) The Crab Nebula, I A U Symp No 46 PP 12-21,
D Reidel, Dordrecht.
- 9) J A Galt and A G Lyne; (1972) Mon Not R A S 158, 281.
- 10) M S Ewing, R A Batchelor, R D Friefeld, R M Price and D H Staelin;
(1962) Ap J Lett L169.
- 11) R B Hanson; (1979) Mon Not R A S 186, 257.
- 12) A G Lyne; (1980) Pulsars, I A U Symp No 95 PP 423-436, B Reidel,
Dordrecht.
- 13) S Chandrasekhar and G Munch; (1950) Ap J 111, 142.
- 14) B M Tinsley; (1980) Found Cosmic Phys 5, 287.

- 15) R Rajamohan; (1978) Mon Not R A S 184, 743.
- 16) P L Bernacca and M Perinotto; (1970) Cont Oss Astro Asiago No 239.
- 17) J P Ostriker and J L Tassoul; (1969) Ap J 155, 987.
- 18) A Slettebak; (1970) Stellar Rotation, Gordon and Breech, New York.
- 19) S Schwarzschild; (1965) Structure and Evolution of Stars, Dover,
New York.
- 20) P Bodenheimer; (1971) Ap J 167, 153.
- 21) A S Endal and S Sofia; (1978) Ap J 220, 279.
- 22) A S Endal and S Sofia; (1979) Ap J 232, 531.
- 23) A S Endal and S Sofia; (1977) Phys Rev Lett 39, 1429.
- 24) L Mestel; (1981) Private Communication.
- 25) S Shapiro; (1979) Source of Gravitational Radiation, PP 355-382,
Cambridge Univ Press, Cambridge.
- 26) D Kazanas; (1977) Nature Lond 267, 501.
- 27) E M Butterworth and J R Ipser; (1976) Ap J 204, 200;

CHAPTER III GRAVITATIONAL COLLAPSE AND GRAVITATIONAL RADIATION

3.1 Introduction

The existence of gravitational waves is one of the characteristic features of the relativistic theory of gravity. Due to the weakness of gravitational coupling and to the quadrupolar nature of gravitational waves, the radiation power of a matter with normal size is usually very small. To have an idea about its weakness, a huge rotating steel bar has been considered¹. Suppose a steel bar having a radius $r=1\text{m}$ and a length $\ell=20\text{m}$, then its mass $M=490\text{tons}$. When it rotates about its middle point with an angular velocity $\omega=28\text{s}^{-1}$, which is the limit to be sustained by its tensile strength, the gravitational radiation power in this case is only $2.2 \cdot 10^{-22} \text{ ergs}^{-1}$. Hence the proof of the existence of gravitational waves cannot be expected to be done by an experiment in the laboratory. The only way is to detect the gravitational waves emitted by astrophysical sources. Among astrophysical source, compact objects are more relevant, since a drastic change of mass distribution can happen only within these objects. For example, a normal close binary system with $m_1 \approx m_2 \approx 1 M_\odot$ has a period of the order of a day and the luminosity of its gravi-

tational radiation is about 10^{30} ergs⁻¹. Instead, a close binary system of neutron stars may have a period of the order of seconds and its luminosity can reach 10^{45} ergs⁻¹. Therefore, gravitational waves are often expected to play an important role in the processes of compact objects, notwithstanding that they have not yet been detected directly.

The collapse of a stellar core is just a drastic dynamical process of compact objects. People usually think that a strong burst of gravitational waves would be radiated during the collapse and that the gravitational radiation in turn, would have prominent effect on the process of collapse. In the last ten years, this problem has been studied quantitatively. Most detailed studies have been done by Saenz and Shapiro^{2,3,4} on the post Newtonian level and by assuming an ellipsoidal shape. They are mainly interested in radiative power and spectrum in order to advise detective works. However, for the ellipsoids with $a \neq b \neq c$, they have also calculated the angular momentum loss by gravitational radiation and found a very small value of $\frac{\Delta J}{J}$. That is the only work which is dealing with the angular momentum loss due to gravitational radiation, nevertheless, we suspect that it is underestimated. In fact, it is better to have an optimistic estimation for our purpose. This forms the motivation of the work presented in

this chapter. The idea of modelling is explained in Section 3.2. The model calculation is done in Section 3.3. A discussion on the results of this model is given in Section 3.4. Finally in Section 3.5, a more general consideration about the change rate of a/m due to gravitational radiation is presented.

3.2 The Idea of Modelling

Now we consider the problem of energy and angular momentum carried by gravitational radiation. The energy formula of quadrupolar radiation was first studied by Einstein⁵ himself in 1918, by using a linearized theory augmented by energy momentum pseudo-tensor of waves. In 1941, Landau and Lifshitz⁶ showed that Einstein's formula is valid also for slow motion sources with Newtonian internal gravity. In 1964, Peters⁷ derived the angular momentum formula of quadrupolar radiation under the same assumptions. Recently, Thorne⁸ systematically studied the multipole expansions of gravitational radiation and showed that ~~qua-~~ for slow motion sources with arbitrarily strong internal gravity, the quadrupole terms of the general formula are the same as those derived by his predecessors. Adopting the $c=G=1$ geometrized unit system, these quadrupole formulas can be written as follows.

$$(3.1) \quad \frac{dE}{dt} = -\frac{1}{5} \langle \ddot{D}_{jk} \ddot{D}_{jk} \rangle$$

$$(3.2) \quad \frac{dJ_i}{dt} = -\frac{2}{5} \langle \ddot{D}_{jl} \ddot{D}_{lk} \rangle \epsilon_{ijk}$$

where D_{jk} is called reduced quadrupolar moment, which can be expressed as integrals over the source⁸.

$$(3.3) \quad D_{jk} = \int \rho \left(x_j x_k - \frac{1}{3} \delta_{jk} x_i x_i \right) d^3x$$

the bracket in (3.1) and (3.2) stand for an average over several wave lengths, all the Latin indices run from 1 to 3, and summation conven-

tion is also used.

Eqs. (3.1)-(3.3) tell us that for slow motion sources the energy and angular momentum carried away by their gravitational radiation can be evaluated by the changing rate of the quadrupolar moment of the source. This task is by no means easy, on the contrary, it is actually very complicated, since, in general, the relativistic dynamical equations of the source are complicatedly mixed with radiative effects. In the post-Newtonian case, the situation is somehow simpler, because radiative effects in this case can be expressed by an additional "radiative reaction potential"⁹

$$(3.4) \quad \phi_{\text{react}} = -\frac{1}{5} \frac{d^5 D_{jk}}{dt^5} x_j x_k$$

and dynamical equations of fluid is simply the classical Euler equation plus the term contributed by radiative reaction potential:

$$(3.5) \quad \rho \frac{dv_i}{dt} + \frac{\partial p}{\partial x_i} - \rho \frac{\partial \phi}{\partial x_i} - \rho \frac{\partial \phi_{\text{react}}}{\partial x_i} = 0$$

where ϕ is the Newtonian potential.

Ignoring the term of radiative reaction potential, the motion of a rigidly rotating homogeneous ellipsoid as a classical problem has been studied very well. There is an exhaustive book on this subject, entitled "Ellipsoidal Figures of Equilibrium", written by Chandrasekhar.¹⁰

If the radiative effect is included, the ellipsoids lose energy and

angular momentum; thus the configuration is no more steady, and in fact, it evolves. Evolving ellipsoidal models were first employed to compute the gravitational radiation by Thuan and Ostriker¹¹ in 1974. Their models are homogeneous, uniformly rotating spheroids with no internal pressure. They considered the models collapse from $\varrho = 0$ till it flattens to a pancake of zero thickness. Afterwards, several improvements have been made. As the internal pressure effect had been included, an interesting feature was found by Shapiro¹² that for a configuration of a given mass and specific entropy, there exists a critical angular momentum J_c for which the energy emission achieves a maximum and decreases for both larger and smaller values of J . This feature is very similar to a well known character of classical spheroids, which says that when J exceeds some critical value the angular velocity ω decreases with an increasing J and finally tends to zero with infinite J (see e.g. Tassoul's book¹³).

The above mentioned studies are all related to axisymmetric cases (spheroids), thus the angular momentum loss is always zero due to the quadrupole nature of radiation. Therefore it has no direct relation with our purpose. Anyhow, Saenz and Shapiro have paid some attention also to non-axisymmetric ellipsoids. Their results say

that $\frac{A}{J}$ is less or much less than 10^{-4} for all of their models. Then the question arises whether this result can reasonably be accepted. We believe that it is an underestimation, specially for the $J > J_c$ cases, due to the reason that their results are still somehow related to the above mentioned classical feature of ellipsoids. If we assume a reasonable deformation for large J cases, the angular velocity will be larger than that of Shapiro's models. Then, the result on gravitational radiation can be expected to be very different since it is very sensitive to the rapidity of rotation.

3.3 A Fast Rotating Non-axisymmetric Model

We consider the gravitational radiation from a homogeneous ellipsoid which is rotating along its z axis with angular velocity ω . The quadrupole moment of a homogeneous ellipsoid with $a \neq b \neq c$ can be expressed referring to its own principal axes as follows

$$(3.6) \quad D_{i'j'} = \begin{pmatrix} D_{x'x'} & 0 & 0 \\ 0 & D_{y'y'} & 0 \\ 0 & 0 & D_{z'z'} \end{pmatrix}$$

where

$$(3.7) \quad \begin{aligned} D_{x'x'} &= \frac{M}{15} (2a^2 - b^2 - c^2) \\ D_{y'y'} &= \frac{M}{15} (2b^2 - c^2 - a^2) \\ D_{z'z'} &= \frac{M}{15} (2c^2 - a^2 - b^2) \end{aligned}$$

and M is the mass of the ellipsoid. The quadrupole moment tensor referred to spatially fixed coordinates can be obtained by the following transformation,

$$(3.8) \quad A_{i,i'} = \begin{pmatrix} \cos\varphi & -\sin\varphi & 0 \\ \sin\varphi & \cos\varphi & 0 \\ 0 & 0 & 1 \end{pmatrix}$$

where φ is the rotating angle. Then,

$$(3.9) \quad D_{ij} = A_{i,i'} A_{j,j'} D_{i'j'} = \begin{pmatrix} D_{xx} & D_{xy} & 0 \\ D_{yx} & D_{yy} & 0 \\ 0 & 0 & D_{zz} \end{pmatrix}$$

where

$$(3.10) \quad \begin{aligned} D_{xx} &= \bar{D} + D_0 \cos 2\varphi \\ D_{yy} &= \bar{D} - D_0 \cos 2\varphi \end{aligned}$$

$$D_{zz} = D_{zz'}$$

and

$$(3.11) \quad \begin{aligned} \bar{D} &= \frac{D_{xx'} + D_{yy'}}{2} = \frac{M}{30} (a^2 + b^2 - 2c^2) \\ D_0 &= \frac{D_{xx'} - D_{yy'}}{2} = \frac{M}{10} (a^2 - b^2) \end{aligned}$$

This rotator is assumed to be a fast one, in the sense that the rotational period is shorter than the collapsing time. Thus the changing rate of the quadrupole moment is only contributed by the rate of φ , and those part contributed from slowly varying parameters a , b and c can be ignored (this is the adiabatic approximation of classical mechanics). Under this assumption, energy and angular momentum losses can be evaluated by (3.1) and (3.2).

$$(3.12) \quad \frac{dM}{dt} = -\frac{1}{5} (\ddot{D}_{xx}^2 + \ddot{D}_{yy}^2 + 2\ddot{D}_{xy}^2) = -\frac{128}{5} D_0^2 \omega^6$$

$$(3.13) \quad \frac{dJ}{dt} = -\frac{2}{5} (\ddot{D}_{xx}\ddot{D}_{yx} + \ddot{D}_{xy}\ddot{D}_{yy} - \ddot{D}_{yx}\ddot{D}_{xx} - \ddot{D}_{yy}\ddot{D}_{yx}) = -\frac{128}{5} D_0^2 \omega^5$$

where $\dot{\omega}$ and $\ddot{\omega}$ has also been neglected.

The quantity which we are interested in is the changing rate of a/m which depends on both $\frac{dM}{dt}$ and $\frac{dJ}{dt}$. From (3.12) and (3.13), we get

$$(3.14) \quad \frac{1}{(\frac{a}{m})} \frac{d(\frac{a}{m})}{dt} = \frac{1}{J} \frac{dJ}{dt} - \frac{2}{M} \frac{dM}{dt} = -\frac{25}{8} \epsilon^2 \left(\frac{a}{m}\right)^4 \left(\frac{r}{r_g}\right)^{-5} \frac{1}{r} + \frac{125}{32} \epsilon^2 \left(\frac{a}{m}\right)^6 \left(\frac{r}{r_g}\right)^{-7} \frac{1}{r}$$

where $\epsilon \equiv \frac{a^2 - b^2}{a^2 + b^2}$, $r \equiv \frac{a^2 + b^2}{2}$ is the averaged square radius of the

equator and $r_g \equiv 2M$ is the gravitational radius. Defining $v \equiv -\frac{dr}{dt}$ as a parameter characterizing the speed of collapse, (3.14) can be written in a dimensionless form.

$$(3.15) \quad \frac{d(\frac{a}{m})}{d(\frac{r}{r_g})} = \frac{25}{8} \epsilon^2 \left(\frac{c}{v}\right) \left(\frac{a}{m}\right)^5 \left(\frac{r}{r_g}\right)^{-6} - \frac{125}{32} \epsilon^2 \left(\frac{c}{v}\right) \left(\frac{a}{m}\right)^7 \left(\frac{r}{r_g}\right)^{-8}$$

Here $1/v$ is written as c/v , in order to show explicitly that it is dimensionless. Formula (3.15) describes how a/m varies with the collapsing radius r/r_g . It is just the point which we are interested in.

The quantities ϵ and v involved in (3.15) are variables. How should we treat them? From the structure of equation (3.15) we see, the changing rate of a/m will differ considerably from zero only in the late stage of collapse ($r/r_g \lesssim 10$). The values of ϵ and v in the early stage will not affect the result. Therefore we can consider ϵ and v as constants and take the value of the late stage for them. The velocity of collapse in the late stage is reasonably estimated as $v/c=0.01$, as the effect of internal pressure has already been taken into account (see e.g. Muller and Hillebrandt¹⁴). The deformation parameter ϵ is taken as $\epsilon^2=0.3$ (i.e. $\frac{b^2}{a^2}=0.3$ and equivalently $e=0.84$), since we want to have a highly deformed model. Substituting these values into (3.15), we get an ordinary differential equation.

$$(3.16) \quad \frac{d(\frac{a}{m})}{d(\frac{r}{r_g})} = \frac{375}{4} \left(\frac{a}{m}\right)^5 \left(\frac{r}{r_g}\right)^{-6} - \frac{1875}{16} \left(\frac{a}{m}\right)^7 \left(\frac{r}{r_g}\right)^{-8}$$

The initial radius $\left(\frac{r}{r_g}\right)_0$ can be taken as 300 which is evaluated from the initial density ρ_0 as to be $3 \cdot 10^9 \text{ gcm}^{-3}$. Later on we will see, the solution of this equation is not sensitive to the initial value. The equation (3.16) has been solved numerically for three values of initial a/m which are 10, 5 and 1. The results are shown in Figure 3.1. The interesting features of the solutions are mainly two. First, at the early stage, a/m almost does not change; rapid reduction of a/m happens at the late stage. Second, when $\frac{r}{r_g}$ reaches 3 which is the radius of a neutron star, the final values of a/m are about 1 in all three cases. Due to this fact we have said in Chapter II that one may expect one order reduction of a/m from gravitational radiation.

3.4 Implication of the Model

We recall that the main assumptions involved in the model are the following two. First, at the late stage of collapse, the stellar core can have both a large angular velocity and a moderately high deformation. Second, at that time, the change of quadrupole moment is mainly due to rotation. If these assumptions are roughly valid, we want to show what the results imply.

From Figure 3.1 we see, the final value of a/m is nearly 1 for all our cases. This behavior is in fact due to the structure of the basic formulas (3.12) and (3.13) in which changing rates of J and M have a high power dependence on ω . Therefore, whenever our assumptions hold true approximately, this feature will probably occur. Then an implication follows. A newly formed neutron star will have a value of a/m larger than the observed value for two to four orders of magnitude. The transformation of rotational energy into electromagnetic radiation is not an enough efficient mechanism for such a reduction as shown in Chapter II. Another more efficient mechanism must therefore be found. We consider it serves as an evidence in support of the Harrison-Tademaru's effect (see Chapter II).

Another implication is related with the instability of collapsing

objects. We still use the parameter τ (defined as the ratio of rotational energy to potential energy) which is related with a/m in our case as

$$(3.17) \quad \left(\frac{a}{m}\right)^2 = \frac{24}{25} \frac{r}{r_g} \tau$$

For a stationary configuration, the instability occurs at $\tau \gtrsim 0.2$.¹³

If a precollapse configuration has initial values $\left(\frac{a}{m}\right)_0 = 10$ and $\left(\frac{r}{r_g}\right)_0 = 300$ as used for our model, formula (3.17) shows that it is almost unstable.

Moreover, the model solution suggests a constancy of a/m from $\frac{r}{r_g} = 300$

to $\frac{r}{r_g} = 20$. When the ratio a/m starts to reduce, the parameter τ of

the configuration reaches a value as high as 5. This value would mean

a serious instability for a stationary configuration, but for a dynamical configuration what would be the consequence? We suspect the

fragmentation will occur and the scenario of collapse will be changed

completely. Fragmented pieces will spiral around their centre of mass,

radiate a burst of gravitational waves and finally fall to form a

neutron star or a black hole. In this scenario, almost all crucial

questions are left unanswered. What is the criterion of the instability

of a dynamical system? What is the timescale of spiralling collapse?

What amount of gravitational waves will be radiated? Will the bounce

still occur in order to induce the supernovae explosion? Probably,

this scenario will not lead to a neutron star formation, for example, due to that the spiralling time of fragmented pieces might be longer than the falling time of the envelope, then the total mass of the finally collapsed object will certainly be larger than the critical mass. Therefore, for the cases of neutron star formation, the value of a/m of a precollapse configuration should not be too much larger than 1 in order to avoid the fragmentation. We think this is another interesting implication from our modelling solution and it is quite noticable in the study of the post main-sequence evolution of a rotating star.

3.5 General Consideration on the a/m Change due to Gravitational Radiation

As it is usually believed, during the collapse of a stellar core, a burst of gravitational waves is radiated out and some amount of angular momentum is carried away. Here we want to emphasize an interesting point that it does not mean the ratio a/m will certainly be reduced.

As we have seen, the change rate of ratio a/m contains two terms.

Now we write it in the following way:

$$\begin{aligned}
 (3.18) \quad \frac{d(\frac{a}{m})}{dt} &= (\frac{a}{m}) \left(\frac{1}{J} \frac{dJ}{dt} - \frac{2}{M} \frac{dM}{dt} \right) \\
 &= (\frac{a}{m}) \frac{1}{J} \frac{dJ}{dt} \left(1 - \frac{2 \frac{dM}{dt} / \frac{dJ}{dt}}{1/a} \right)
 \end{aligned}$$

Both factors $2 \frac{dM}{dt} / \frac{dJ}{dt}$ and $1/a$ have the dimension as a frequency, therefore we call $1/a$ as the critical frequency Ω_c which depends on the instantaneous configuration of the source and call $2 \frac{dM}{dt} / \frac{dJ}{dt}$ as frequency Ω which depends on the dynamical process of radiation. If Ω is larger than Ω_c , it is the case of mass loss dominant, therefore the ratio a/m is increasing, despite of the fact that angular momentum is reducing.

Consider the stellar core collapse as an example. The critical frequency Ω_c depends on the mass m and the ratio a/m . Assuming

$m = 1M_{\odot} = 5 \cdot 10^{-6}$ sec, we have the value of Ω_c ,

$$(3.19) \quad \begin{aligned} \Omega_c &= 10^5 \text{ sec}^{-1} & \text{for } \frac{a}{m} &= 1 \\ \Omega_c &= 10^4 \text{ sec}^{-1} & \text{for } \frac{a}{m} &= 10 \end{aligned}$$

It is just about the typical frequency of neutron star or black hole processes. Moreover we use this idea in connection with the above discussed model. From (3.12) and (3.13) we find that the frequency Ω defined in this section is equal to 2ω which is exactly the frequency of radiation. Thus the point is to compare the radiative frequency with the critical frequency. It can be proved that the mass loss dominant case would happen if $\omega r > \frac{\sqrt{5}}{2} c$. In fact this is impossible. As we see, the calculating result has shown that in this case, angular momentum loss is dominant. The ratio a/m is decreased due to gravitational radiation.

Generally, for a periodical or quasi-periodical process, such as rotation, revolution, vibration, spiral motion etc., the criterion of whether the angular momentum loss or the mass loss is dominant, can be analysed as follows.

In these cases, there must be a main frequency ω , then the change of quadrupole moment can be expressed as follows.

$$(3.21) \quad D_{ij} \sim \bar{D} + D_0 e^{i\omega t}$$

where the sign " \sim " means "by the order of magnitude they are equal".

Then, by the same approximation, we have

$$(3.22) \quad \begin{aligned} \ddot{D} &\sim \omega^2 D_0 \\ \dddot{D} &\sim \omega^3 D_0 \end{aligned}$$

From (3.1) and (3.2), it leads to

$$(3.23) \quad \begin{aligned} \frac{dM}{dt} &\sim \frac{1}{5} \omega^6 D_0^2 \\ \frac{dJ}{dt} &\sim \frac{2}{5} \omega^5 D_0^2 \end{aligned}$$

and consequently,

$$(3.24) \quad \Omega \equiv 2 \frac{\frac{dM}{dt}}{\frac{dJ}{dt}} \sim \omega$$

This formula says that Ω is of the same order of magnitude of the main frequency ω in the dynamical process. The difference between Ω and ω derives from two reasons. First, the amplitude of the diagonal elements D_{ii} , which contribute only to $\frac{dM}{dt}$, may be different from that of the off-diagonal elements D_{ij} , which contribute to both $\frac{dM}{dt}$ and $\frac{dJ}{dt}$. Second, the sum in the expression of $\frac{dM}{dt}$ (see (3.1)) may contain more terms than that in the expression of $\frac{dJ}{dt}$ (see (3.2)), since $\frac{dJ}{dt}$ is only contributed by off-diagonal terms. Finally, we conclude as follows. When the main frequency ω of the dynamical process is much larger than Ω_c , the ratio a/m would not be reduced, although a certain amount of angular momentum is carried away. As far as the a/m issue is concerned, however, this point is worthy to be noticed.

References for Chapter III

- 1) C W Misner, K S Thorne and J A Wheeler; (1973) Gravitation, W H Freeman & Co..
- 2) R A Saenz and S L Shapiro; (1978) Ap J 221, 286.
- 3) R A Saenz and S L Shapiro; (1979) Ap J 229, 1107.
- 4) R A Saenz and S L Shapiro; (1981) Ap J 244, 1033.
- 5) A Einstein; (1918) Preuss Akad Wiss, Berlin, Sitzber, 154.
- 6) L D Landau and E M Lifshitz; (1941) Teoriya Polya, Nauka, Moscow.
- 7) P C Peters; (1964) Phys Rev B136, 1224.
- 8) K S Thorne; (1980) Rev Mod Phys 52, 299.
- 9)
- 10) S Chandrasekhar; (1969) Ellipsoidal Figures of Equilibrium, Yale Univ Press.
- 11) T X Thuan and J P Ostriker; (1974) Ap J Lett 191, L105.
- 12) S L Shapiro; (1977) Ap J 214, 566.
- 13) J L Tassoul; (1978) Theory of Rotating Stars Chap 4, Princeton Univ Press.
- 14) E Muller and W Hillebrandt; (1981) Astron Astrophys 103, 358.

CHAPTER IV GRAVITATIONAL COLLAPSE AND NEUTRINO PROCESSES

4.1 Introduction

The importance of neutrino processes in gravitational collapse can simply be understood. In forming a neutron star with $1M_{\odot}$, a total amount of energy of about 10^{53} ergs must be radiated out according to the virial theorem. On the other hand, in order to neutronize the whole star, about 10^{57} protons must transform into neutrons and 10^{57} neutrinos are to be emitted. On the average, each neutrino would carry away the energy of about 16MeV (i.e. $3 \cdot 10^{-5}$ erg). Thus, about $3 \cdot 10^{52}$ ergs are carried away by neutrinos produced in the neutronization process. In fact, the neutrino emission is the main process in carrying away the energy and making the collapse to be able to continue. Besides, it also affects almost all other aspects of the collapse, due to the fact that neutrinos are the main energy carrier. For example, let us see the problem of rotation. Because neutrinos do not carry away a large amount of angular momentum, we have not paid much attention to them in our previous consideration, but neutrino processes are still quite relevant in this problem, due to the fact that neutrino emission can damp out pulsations¹ then reduces the gravitational radiation which is probably

the main carrier of angular momentum. It is not exaggerated to say that neutrino processes are the most important processes involved in gravitational collapse.

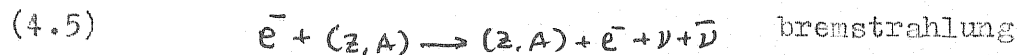
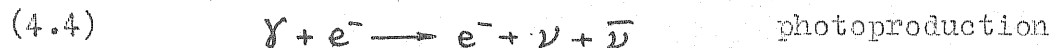
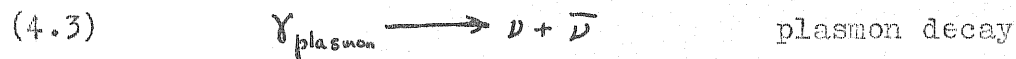
Neutrino processes can be divided into two categories: neutrino production and neutrino transportation. The mechanisms of neutrino production are neutronization (also called electron capture):



due to the high Fermi energy of degenerated electron gas and thermal production which mainly takes place via



where electron-positron pair come from photoproduction due to high temperature, and also via



The neutronization rate sensitively depends on the chemical compositions. Since chemical compositions change rapidly, a definite result is rather difficult to be reached. The thermal production rates sensitively depend on the density and temperature, which are both very high. In this case, a dynamical process such as pulsation can

change the rate prominently¹. Therefore the quantitative results rely on the model and far from conclusive.

Neutrino transportation is the main subject of this chapter. It is a delicate problem related to final states of collapse. First, we review the recent idea about neutrino trapping due to weak interaction in Section 4.2. Another neutrino trapping mechanism due to strong gravitational field is presented in Section 4.3. In Section 4.4 we discuss physical effects of purely gravitational trapping.

4.2 The General Problem of Neutrino Trapping

It was Gamow et al.² who first pointed out in 1941 that neutrinos may play an important role in the stellar evolution. Owing to the weakness of interaction between neutrinos and matter, neutrinos escape from stellar core instantaneously as it is produced and carry away energy and momentum; thus they speed up the process of evolution. Actually, During the H and He burning stages, neutrinos are produced by thermal nuclear reactions, ~~but~~ they are not very energetic. Starting from carbon ignition, temperature grows so high that thermal production of neutrinos becomes significant, then the energy carried away by neutrinos comes to be ^{so} large that qualitative features and timescales of latter stages of stellar evolution are prominently affected. However, the stellar matter is not always transparent for neutrinos. It gradually turns to be opaque while the density becomes higher and higher. Consequently, after a neutrino is produced, it diffuse out instead of escape. By other words, part ^{of} neutrinos is held up in the stellar matter. That is what we called neutrino trapping.

Transparency of the core matter to neutrinos can be characterized by the relative size of neutrino mean free path λ with the radius R of the core. The core can be called a transparent one if $\lambda \gg R$ and

is opaque if $\lambda \ll R$. The mean free path λ is determined by the composition, density and temperature of the core matter and neutrino energy. For a 20MeV neutrino (or antineutrino) moving in a free proton neutron and electron gas, the mean free path has been evaluated as $\lambda \approx 10^{17} g^{-1} cm^3$. For a precollapse core with $M=1.4M_{\odot}$ and $\rho \approx 3 \cdot 10^9 g cm^{-3}$, R is about $2 \cdot 10^7 cm$; λ is about $3 \cdot 10^7 cm$. Therefore they are of the same order. This shows that we must consider the collapsing core as an opaque object to neutrinos.

From a microscope viewpoint, neutrino opacity comes from the interaction of neutrino with other particles, thus the available mechanism depends on the theory of interaction. In the old time, the weak interaction was considered to proceed only via charged currents which was first suggested by Fermi⁴ in dealing with β decay of nuclei. Neutral current processes was not discovered till 1973⁵. Soon after, Weinberg⁶ and Salam⁷ theory of unified weak-electromagnetic interaction was proved to be a correct framework for studying weak interaction processes including those involving weak neutral currents. Since then, people have had a good basis to work on with the neutrino processes in particle physics and astrophysics as well. According to the old theory, neutrino opacity derived from two sources:

$$(4.6) \quad e^- + \nu_e \rightarrow \nu_e + e^- \quad e^- - \nu_e \text{ scattering}$$

$$(4.7) \quad \nu_e + n \rightarrow p + e^- \quad \nu_e \text{ recapture}$$

The corresponding Feynman diagram are shown in Figure 4.1 (1) and (3). Because of the degeneracy of electrons, process (4.6) is more effective than (4.7). Including neutral current, $e^- - \nu$ scattering is strengthened by a new mechanism shown in Figure 4.2 (2); and $\nu - n$ scattering as shown in Figure 4.1 (4) becomes possible.

$$(4.8) \quad \nu + n \rightarrow n + \nu \quad \nu - n \text{ scattering}$$

In 1975, Schramm and Arnett⁸ recalculated the neutrino opacity by including the neutral currents. In 1977, Arnett⁹ showed that opacities are too large to allow much transport by neutrinos, about half of them in fact remains within the fluid at the time when the core bounce occurs. Next year, Arnett¹⁰ said in the 9th Texas Symposium on Relativistic Astrophysics: "the shift in emphasis had been away from neutrino 'transport' and towards neutrino 'trapping'."

After finding the neutrino trapping, various consequences have been investigated by several researchers⁹⁻¹³. Some results are really interesting. Since the stellar matter now contain a large amount of neutrinos, the neutrino pressure becomes a significant source in supporting the gravity, therefore the equation of state needs

to be further studied. Another crucial influence is related with the mass ejection. In particular, this problem was considered by Arnett and his collaborators^{9, 11, 14}. They pointed out that if the momentum transfer by neutrinos would induce a mass ejection, the average energy of neutrinos should be larger than 15 MeV. In fact, this is probably the case. Therefore the problem lies in the efficiency of neutrino transportation, i.e. whether neutrinos can diffuse out rapidly enough to the envelope to reach the Eddington limit of neutrino flux at the mantle. Now this is still an open question; because of the strong neutrino trapping, it seems unlikely. Another possible mechanism of mass ejection via the collapse-bounce-shock wave-explosion scenario has also been studied. The results are even more uncertain. Whether or not an explosion follows a collapse, it depends on several factors, specially on the density at which the inner core bounces. This density sensitively depends on how strong neutrinos are trapped. Arnett thought this may explain the diversity of the results obtained from various numerical models. In short, despite of all the uncertainties, it seems clear that neutrino trapping is in fact a delicate factor in the fate of collapsing objects. Therefore, detailed consideration is needed, in order to have convincing results. In the above mentioned works

on neutrino trapping, the effects from the gravitational force are ignored. The gravitational field can trap neutrinos has been shown

by several authors¹⁵⁻¹⁹. Our work contained in following sections is

to show that for massive neutrinos, the gravitational trapping effect

is much stronger than that in the massless neutrino case and also

show that this effect alone is not strong enough to have significant

result. The potentially important consequence might lie in the com-

bining effect of weak interaction trapping and gravitational trapping

which will appear in our further works.

4.3 Gravitational Trapping of Neutrinos[†]

A well known property of a gravitational field in general relativity is to bend lightlike trajectories. If the gravitational field is strong enough, these trajectories can be trapped^{††}, thus massless particles such as photons or neutrinos are prevented from escaping out of the field. In this section, we consider how this effect works inside condensed objects such as neutron stars or collapsing stellar cores.

As for massless neutrinos, the gravitational trapping effect in some interior field has been studied by several authors¹⁵⁻¹⁹. The main features of the trapping effect in the interior Schwarzschild field are two. First, it happens only when the stellar radius is less than $3/2 r_g$, where r_g is its gravitational radius; consequently, it does not happen in a neutron star, since its radius is about $3r_g$. Second, the trapping effect happens only with those neutrinos which have a

[†] The work presented in this and next sections has been published in IL NUOVO CIMENTO 65B, 79 (1981), jointly with F de Felice.

^{††} The meaning of the term "trapping" used here is somehow different from the same word used formerly. Here by "trapping" we mean that trajectories are confined in a finite region.

high angular momentum. As neutrinos might have some rest mass, It is worthy to find out, for massive neutrinos, how the features are modified.

Let us consider a massive neutrino moving in the Schwarzschild interior field, which is described as follows.

$$(4.9) \quad ds^2 = - \left[\frac{3}{2} \left(1 - \frac{2m}{r_0} \right)^{\frac{1}{2}} - \frac{1}{2} \left(1 - \frac{2mr^2}{r_0^3} \right)^{\frac{1}{2}} \right]^2 dt^2 + \left(1 - \frac{2mr^2}{r_0^3} \right)^{-1} dr^2 + r^2 (d\theta^2 + \sin^2 \theta d\varphi^2)$$

for $r \leq r_0$,

where $c=G=1$ geometrized units are used. The equation of motion can be expressed by Hamilton-Jacobi equation

$$(4.10) \quad g^{ij} \frac{\partial S}{\partial x^i} \frac{\partial S}{\partial x^j} + m_\nu^2 = 0$$

where S is called Hamilton principal function and m_ν is the rest mass of a neutrino. Owing to the spherical symmetry and the staticity of the metric (4.9), we can easily obtain a complete set of first integrals from (4.10).

$$(4.11) \quad \begin{aligned} \frac{\partial S}{\partial t} &= E, \\ \frac{\partial S}{\partial \varphi} &= l \\ \frac{\partial S}{\partial \theta} &= \pm \left[L^2 - \frac{l^2}{\sin^2 \theta} \right]^{\frac{1}{2}} \\ \frac{\partial S}{\partial r} &= \pm \left[g_{rr} \left(\frac{E^2}{-g_{tt}} - \frac{L^2}{r^2} - m_\nu^2 \right) \right]^{\frac{1}{2}} \end{aligned}$$

where E , L and l stand for the total neutrino energy, total angular momentum and its φ component. All of them are constants of motion.

If a neutrino is trapped, its trajectory should be bounded and

the maximal radial coordinate satisfies a relation

$$(4.12) \quad m, \frac{dr}{dt} = g^{rr} \frac{\partial S}{\partial r} = 0$$

For simplicity, we introduce a dimensionless quantity

$$(4.13) \quad y = \left(1 - \frac{2Mr^2}{r_0^3}\right)^{1/2}$$

instead of r , as a radial variable. At the edge of the star,

$$(4.14) \quad y_0 = \left(1 - \frac{2M}{r_0}\right)^{1/2}$$

y_0 varies from $1/3$ to 1 corresponding to r varying from $\frac{9}{8}r_g$ to ∞

which is the physical limit of the stellar radius. For a fixed radius

y_0 , y varies from 1 (centre of the star) to y_0 (edge of the star).

From the last equation of (4.11), the relation which should be satisfied by the maximal radius coordinate can be rewritten as

$$(4.15) \quad Y^2 = \frac{1}{4} (3y_0 - y)^2 \left[\Lambda^2 \frac{(1 - y_0^2)^3}{1 - y^2} + 1 \right]$$

where $Y \equiv \frac{E}{m}$ and $\Lambda \equiv \frac{L}{2mr}$ are dimensionless quantities in place of E

and L . Relation (4.15) can also be rewritten as

$$(4.16) \quad \Lambda^2 = \frac{1 - y^2}{(1 - y_0^2)^3} \left[\frac{4Y^2}{(3y_0 - y)^2} - 1 \right]$$

using (4.15) or (4.16), we are able to answer a) what is the range

of y_0 in which trapping happens? b) for a fixed y_0 , what is the range

of energy Y in which neutrino could be trapped? c) for fixed y_0 and

Y , what is the range of angular momentum Λ in which neutrino are

trapped?

Let us consider a star with fixed radius y_0 . If a neutrino having energy γ can be trapped, there must be a value of y in the range of 1 to y_0 satisfying $\left(\frac{\partial \Lambda^2}{\partial y}\right)_{y_0, \gamma} = 0$. From (4.16), this condition reads

$$(4.17) \quad \gamma^2 = \frac{\gamma_1 (\gamma_1 - 3y_0)^3}{4(1 - 3\gamma_1 y_0)}$$

where y_1 is the radial coordinate corresponding to maximal Λ^2 . Condition (4.17) shows that for any y_0 , we can find a range of γ^2 , corresponding to which some y_1 exists within the stellar radius. Since γ^2 varies with y_1 monotonically, it is easy to find the maximum trapping energy γ_{\max}^2 and minimum trapping energy γ_{\min}^2 for any y_0 .

$$(4.18) \quad \gamma_{\max}^2 = \frac{2y_0^4}{3y_0^2 - 1}$$

$$(4.19) \quad \gamma_{\min}^2 = \left(\frac{3}{2}y_0 - \frac{1}{2}\right)^2$$

Figure 4.2 shows the curves for trapping energy at any radius. The region under the curve of γ_{\min}^2 is in fact unphysical. The range of Λ^2 for trapped neutrinos is expressed in formula (4.16). For fixed y_0 and γ^2 , Λ^2 goes up from zero (at centre, i.e. $y=1$) to Λ_{ext}^2 (at $y=y_1$), then goes down to Λ_0^2 (at stellar surface $y=y_0$). Some typical behaviors are shown in Figure 4.3. Actually, Λ_0^2 determines the range of angular momentum in which neutrinos are trapped. If $\Lambda_0^2 \leq 0$ for some value of γ^2 , it says that at this energy neutrino with any angular momentum are trapped. This case can be called a "complete trap". If $\Lambda_0^2 > 0$,

only those neutrino having the angular momentum $\Lambda_0^2 \leq \Lambda^2 \leq \Lambda_{ext}^2$ are trapped. Thus it is called a "partial trap". From (4.16) we see, the critical value of γ^2 for a complete trap or a partial trap reads

$$(4.20) \quad \gamma_{crit}^2 = \gamma_0^2$$

All the behaviors corresponding to any γ_0 are shown in Figure 4.2.

Some details can be found in the reference.²⁰ Here we summarize the main points as follows.

a) Contrary to the massless neutrino case, gravitational trap of massive neutrinos do exist in any stellar interior, no matter how large its radius is.

b) When $r_0 \leq \frac{3}{2} r_g$ (i.e. $\gamma_0 \leq \frac{1}{3}$), neutrinos with any value of energy can be trapped; when $r_0 > \frac{3}{2} r_g$, the energy of trapped neutrinos is limited in some range shown by (4.18) and (4.19).

c) For some energy γ ranging between γ_{max} and γ_{crit} , neutrinos are partially trapped, in the sense that it can escape by changing its direction of motion but retaining its energy.

d) For some energy γ ranging between γ_{crit} and γ_{min} , neutrinos are completely trapped, in the sense that it can never escape without gaining energy.

4.4 Effects of Gravitational Trapping of Neutrinos in Condensed Objects

It has been shown in the last section that even in a normal star not all the neutrinos produced inside can escape, a fraction of them is in fact retained even if the weak interaction is ignored. Now we consider the case in which the density of stellar matter is larger than 10^7 gm^{-3} , thus the inverse β -decay

$$(4.21) \quad e^- + p \rightarrow n + \nu_e$$

is happening in the star. We want to know, under which condition the gravitational trapped neutrinos would make the inverse reaction equally important.

The rate of neutrino production in process (4.21) is given by

$$(4.22) \quad \frac{d^2 n_\nu}{dt dV} = \frac{d^2 n(p \rightarrow n)}{dt dV} = n_p \int_{\epsilon_n}^{\epsilon_F} \frac{dn_e(\epsilon_e)}{d\epsilon_e} v_e(\epsilon_e) \sigma(\epsilon_e) d\epsilon_e$$

where ϵ_n and ϵ_F are the threshold and Fermi energy of electrons, v_e is their velocity and σ is the cross-section for inverse β -decay.

Here and in what follows the energies ϵ and the velocities v are referred to a local stationary observer. Taking $\sigma \sim 10^{-44} \text{ cm}^2$ as constant and $v_e(\epsilon_e) \sim c$, we have as an estimation

$$(4.23) \quad \frac{d^2 n_\nu}{dt dV} \approx n_p n_e \sigma c$$

The proton and electron densities in (4.22) can be obtained by re-

quiring that the constituents in the neutronization process are in chemical equilibrium. To the first approximation we neglect the neutrino component, so we have

$$(4.24) \quad \sqrt{m_n^2 c^2 + \Lambda^2 n_n^{2/3}} = \sqrt{m_p^2 c^2 + \Lambda^2 n_p^{2/3}} + \sqrt{m_e^2 c^2 + \Lambda^2 n_e^{2/3}}$$

where $\Lambda = \left(\frac{3}{8\pi}\right)^{1/2} h = 3.26 \cdot 10^{-27}$ e.g.s., h being the Planck constant, $n_p = n_e = n_B - n_n = \frac{\rho}{H} - n_n$; here ρ is the matter density, H the proton mass, n_B the baryon number density.

Solving (4.23) numerically, we have

$$(4.25) \quad \begin{aligned} \text{a) for } \rho = 10^{10} \text{ g cm}^{-3}, \quad n_B = 6 \cdot 10^{32} \text{ cm}^{-3} \text{ and } n_p = n_e = 9 \cdot 10^{30} \text{ cm}^{-3} \\ \text{b) for } \rho = 10^{14} \text{ g cm}^{-3}, \quad n_B = 6 \cdot 10^{37} \text{ cm}^{-3} \text{ and } n_p = n_e = 1.3 \cdot 10^{35} \text{ cm}^{-3} \end{aligned}$$

In the above two cases we have

$$(4.26) \quad \begin{aligned} \text{a) } \frac{d^2 n_\nu}{dt dV} &\approx 2 \cdot 10^{28} \text{ cm}^{-3} \text{ s}^{-1} \\ \text{b) } \frac{d^2 n_\nu}{dt dV} &\approx 5 \cdot 10^{36} \text{ cm}^{-3} \text{ s}^{-1} \end{aligned}$$

Then we turn to the induced β -decay (inverse of (4.21))

$$(4.27) \quad \nu_e + n \longrightarrow p + e^-$$

As before, we have

$$(4.28) \quad \frac{d^2 n_\nu(n \rightarrow p)}{dt dV} = n_n \int_{\xi_1}^{\xi_2} \frac{dn_\nu}{d\xi_\nu} \nu_\nu(\xi_\nu) \sigma(\xi_\nu) d\xi_\nu \approx n_n n_\nu \sigma c$$

where ξ_2 and ξ_1 is the upper and lower limit of the local energy of trapped neutrinos, and ν_ν and σ are assumed to be constant again.

The cross-section σ in (4.28) should be nearly equal to that in

(4.23). Therefore, for the induced and the inverse β -decay to become competitive, we need a neutrino concentration

$$(4.29) \quad \begin{aligned} \text{a)} \quad n_\nu &\approx \frac{n_p n_e}{n_n} \approx 10^{28} \text{ cm}^{-3} \\ \text{b)} \quad n_\nu &\approx \frac{n_p n_e}{n_n} \approx 10^{32} \text{ cm}^{-3} \end{aligned}$$

Now let us see how many neutrinos are actually trapped in the star.

Consider a $1M_\odot$ neutron star with a radius $r_0 \approx 1.5 \cdot 10^6 \text{ cm}$ and a density $\rho \approx 10^{14} \text{ gcm}^{-3}$. The hypothesis we make here is that the only neutrinos of interest are those completely trapped and that they should be degenerated. In this case, their number density per unit energy range

$$(4.30) \quad \frac{dn_\nu}{d\varepsilon_\nu} \text{ is fixed by the exclusion principle, namely}$$

$$\frac{dn_\nu}{d\varepsilon_\nu} = \frac{8\pi \varepsilon_\nu^2}{c^3 h^3}$$

Therefore the average number density of trapped neutrino reads

$$(4.31) \quad n_\nu = \frac{8\pi}{3c^3 h^3} (\varepsilon_2^3 - \varepsilon_1^3)$$

The energy ε used here is local energy and it relates to the conserved energy E by

$$(4.32) \quad E = \sqrt{-g_{00}} \varepsilon$$

The metric component g_{00} reads from (4.9) by noting (4.13)

$$(4.33) \quad -g_{00} = \left(\frac{3}{2}y_0 - \frac{1}{2}y\right)^2$$

For $1M_\odot$ neutron star, $r_0 \approx 1.5 \cdot 10^6 \text{ cm}$ means $y_0 \approx 0.9$. When y varies in the stellar interior (i.e. from $y=1$ to $y=y_0$), $-g_{00}$ is always nearly

equal to 1. That is to say that relativistic energy shift is not important in our case, when ^{only} an order of magnitude is concerned. Moreover, we assume an observational upper limit for the electronic neutrino mass

$$(4.34) \quad m_\nu c^2 = 6.0 \cdot 10^{-5} \text{ MeV}$$

consequently, the number density of trapped neutrinos is estimated as to be 10^{17} cm^{-3} which is vanishingly small comparing with (4.29).

However, an interesting result happens from (4.32) and (4.33). If the density of a collapsing object is even denser than that of a neutron star and reaches the limiting case in which $y = 1/3$, (i.e. $r_0 = \frac{9}{8} r_g$, see e.g. de Felice¹⁸), q_{∞} would equal to zero in the center of this configuration. It means that in the central region, the concentration of trapped neutrinos should be very high. Of course, it is not clear that what the realistic analogue of the limiting case of uniform stellar models is.

Finally, as the conclusion of this section we can safely say that the trapping effect of neutrinos from the gravitational force alone is not significant in the process of forming a neutron star, even if the neutrino is massive. This does not mean that it has nothing to do with the issue of final states. On the contrary, if the fate

of collapsing objects in fact delicately depends on the concentration of trapped neutrinos as indicated by Arnett⁹, it might be an important aspect of this issue. Anyhow, the neutrino trapping as discussed by Arnett and his collaborators will be strengthened by the gravitational force and this strengthening is worth of further considerations.

References for Chapter IV

- 1) D Kazanas and D N Schramm; (1977) Ap J 214, 819.
- 2) G Gamow and M Schonberg; (1941) Phys Rev 59, 539.
- 3) D Z Freedman, D N Schramm and D L Tubbs; (1977) Ann Rev Nucl Sci 27, 167.
- 4) E Fermi; (1934) Zeit Phys 88, 161.
- 5) See e g W Lee; (1974) Proc Inter Conf High Ener Phys 17th.
- 6) S Weinberg; (1967) Phys Rev Lett 19, 1264.
- 7) A Salam; (1968) Elementary Particle Physics, Ed N Svortholm, P 367
Stockholm.
- 8) D N Schramm and W D Arnett; (1975) Ap J 198, 629.
- 9) W D Arnett; (1977) Ap J 218, 815.
- 10) W D Arnett; (1980) Ann N Y Acad Sci 336, 366.
- 11) K A Van Riper and W D Arnett; (1978) Ap J 225, L129.
- 12) J R Wilson; (1980) Ann N Y Acad Sci 336, 358.
- 13) W D Arnett; (1979) Sources of Gravitational Radiation, P 311,
Ed L Smarr, Cambridge Univ Press, Cambridge.
- 14) S W Brueun, W D Arnett and D N Schramm; (1977) Ap J 213, 213.
- 15) B Kuchowicz; (1974) Gen Rel Grav 5, 201.
- 16) F de Felice; (1969) Nuo Cim 63B, 649.

- 17) P Collas and J K Lawrence; (1976) Gen Rel Grav 7, 715.
- 18) S N Guha Thakurta; (1978) J Phys A 11, 2213.
- 19) A K Kembhavi and C V Vishveshwara; (1980) Phys Rev D22, 2349.
- 20) F de Felice and Y Yu; (1981) Nuovo Cim 65B, 79.

5.1 Introduction

As well known, a black hole, in general, can be both charged and rotating, however, it must satisfy a constraint

$$(1.3) \quad M^2 \geq a^2 + Q^2$$

This constraint tells that the collapsing star should neither rotate too fast nor be too much charged in order to be able to form an event horizon. Otherwise, the singularity at $R=0$ will be naked.

As mentioned in Chapter I, the reality of the naked singularity is still a controversial problem. To study the physical process of collapse as we have done in the previous chapters is one way to find some hint to this problem. Now we intend to study the same problem from another angle. That is to consider the phenomenological similarity and dissimilarity between black holes and naked singularities, by assuming their existence in nature a priori. Several years ago, de Felice¹ studied the phenomenon of Kerr naked singularities (rotating but uncharged), and pointed out that as far as the optical appearance is concerned, a naked singularity is undistinguishable from a black hole, in the sense that photons emitted from the singularities are also infinitely redshifted. It implies that a naked singularity

is in fact invisible, just like a black hole.

The work contained in this chapter is devoted to the collapse of non-rotating charged stars, but only their optical appearance is concerned. The possible cases are divided into two categories. The continuous collapse towards an event horizon ($Q \leq M$ cases) or a naked singularity ($Q > M$ cases) is in Section 5.4. Another category considered in Section 5.5 is the vibrating charged stars (also $Q > M$ cases), which will be argued as the most probable configuration of a collapsing, overcharged star. Before the study of these cases, we need some preparation. The dynamical behavior of the surface of a collapsing charged star is dealt with in Section 5.2. On the other hand, the behavior of photons in the gravitational field of a charged star (Reissner-Nordstrom field^{2,3}) is considered in Section 5.3. Later on we will see that the optical similarity of a naked singularity to a black hole in the Reissner-Nordstrom case is the same as that in the Kerr case, i.e. ~~a~~naked Reissner-Nordstrom singularity is also invisible. Its luminosity is asymptotically vanished and its color is infinitely redshifted. Besides, also some other interesting features are revealed. All results are finally summarized in the last section 5.6.

Before going on, there is still one point worthy to be mentioned. Usually, it is not thought that a charged star could be realized, specially an overcharged one ($Q > M$). In fact, the $Q=M$ case means that one charged baryon out of 10^{16} baryons is not electrically balanced. It is not an inconcievably large amount. Anyhow, to prove the reality of a highly charged star is out of our intention. For us, the compelling point is only the fact that the charged star is one of few cases allowed for studying naked singularities.

5.2 Collapse of Charged Stars

Let us study the collapse of a spherical, pressureless, non-rotating and charged star (i.e. a charged dust ball). The surface of the star moves along radial geodesic lines and the inner part is assumed to be maintained inside. The Jacobi-Hamilton equation for a mass element moving in the gravitational field and electromagnetic field, in general takes the form

$$(5.1) \quad g^{ij} \left(\frac{\partial S}{\partial x^i} - e A_i \right) \left(\frac{\partial S}{\partial x^j} - e A_j \right) = -\mu^2$$

where e and μ are the charge and mass of the moving element respectively, A_i is the electromagnetic potential and in our case reads

$$(5.2) \quad \begin{aligned} A_0 &= Q/R, \\ A_\mu &= 0 \quad \text{for } \mu = 1, 2, 3; \end{aligned}$$

and g^{ij} is the metric. The Reissner-Nordstrom metric can be read from

$$(5.3) \quad ds^2 = g_{ij} dx^i dx^j = - \left(1 - \frac{2M}{R} + \frac{Q^2}{R^2} \right) dt^2 + \left(1 - \frac{2M}{R} + \frac{Q^2}{R^2} \right)^{-1} dR^2 + R^2 (d\theta^2 + \sin^2 \theta d\varphi^2)$$

where Q and M are the charge and mass of the whole star respectively.

We remind that Jacobian principal function S in these cases is related with the generalized velocities as follows.

$$(5.4) \quad \frac{\partial S}{\partial R} = P_R = g_{RR} \dot{R} = \mu g_{RR} \frac{dR}{d\tau}$$

$$(5.5) \quad \frac{\partial S}{\partial t} = P_t = E$$

where E is the conserved energy of a testing particle. The dynamical

equation of a radially moving particle then can be derived from (5.1)-(5.5).

$$(5.6) \quad \left(\frac{dr}{dt}\right)^2 = \left(\tilde{\epsilon} - \frac{\tilde{e}Q}{R}\right)^2 - \left(1 - \frac{2M}{R} + \frac{Q^2}{R^2}\right)$$

where $\tilde{\epsilon} \equiv \frac{\epsilon}{\mu}$ and $\tilde{e} \equiv \frac{e}{\mu}$ called specific energy and specific charge respectively. It is helpful to define a "potential" $V(R)$, as if $\frac{dr}{dt} = 0$, then it equals to the specific energy $\tilde{\epsilon}$.

$$(5.7) \quad V(R) = \sqrt{1 - \frac{2M}{R} + \frac{Q^2}{R^2}} + \frac{\tilde{e}Q}{R}$$

The minus sign of the square root has been ignored in (5.7), since it describes the behavior of antimatter. From (5.7) we see that the shape of potential not only depends on the stellar parameters M and Q , but also on the particle's parameter \tilde{e} .

Figure 5.1 shows the potential curves for the $\frac{Q}{M} < 1$ case (Q is assumed to be positive). When $\tilde{e} < \frac{M}{Q}$, the configuration can be equilibrated due to the pressure gradient. When $\tilde{e} > \frac{M}{Q}$ the configuration can be equilibrated only at $R < R_{\max}$ (see Figure 5.1). Otherwise, the electrically repulsive force is dominating, thus it is impossible to have an equilibrium state. For the cases that equilibrium configurations do exist, a charged star can collapse too, as if the pressure is suddenly reduced. The collapsing surface will pass through the event horizon at $R = R_+$, but the phenomenon which

can be seen by a distant observer is only related with $R > R_+$ region.

All these qualitative features are the same as those in the Schwarzschild case.

Since we are interested in the optical appearance relative to a distant observer, the coordinate velocity is a more relevant quantity.

From

$$(5.8) \quad \frac{dt}{d\tau} = \left(1 - \frac{2M}{R} + \frac{Q^2}{R^2}\right)^{-1} \left(\tilde{E} - \frac{\tilde{E}Q}{R}\right)$$

the coordinate velocity reads

$$(5.9) \quad \frac{dR}{dt} = \frac{\frac{dR}{d\tau}}{\frac{dt}{d\tau}} = -\left(1 - \frac{2M}{R} + \frac{Q^2}{R^2}\right) \sqrt{1 - \frac{1 - \frac{2M}{R} + \frac{Q^2}{R^2}}{\left(\tilde{E} - \frac{\tilde{E}Q}{R}\right)^2}}$$

This velocity tends to zero when the star collapses towards the event horizon.

Figure 5.2 shows the potential curves for the $\frac{Q}{M} > 1$ cases. The behavior of the star in these cases is somewhat complicated. When the specific charge \tilde{e} at the surface is less than -1 , the star may have an equilibrium configuration at any radius, and once it collapses, it proceeds towards the singularity at $R=0$. On the contrary, when $\tilde{e} > \frac{M}{Q}$, neither equilibrium nor collapse happens. Moreover, due to the presence of an infinitely hard repulsive core, the singularity will never be reached by any test particle. The mediate case $-1 < \tilde{e} < \frac{M}{Q}$ is the most interesting one. Since the net force is attractive for

$R > R_{ext}$ and is repulsive for $R < R_{ext}$, the equilibrium state can exist only at $R > R_{ext}$. Once it collapses, it will oscillate.

5.3 Motion of Photons in the Reissner-Nordstrom Field

The equations of motion of photons in the Reissner-Nordstrom field can be derived from the Jacobi-Hamilton equation by considering that t , θ and φ are cyclic coordinates.

$$(5.10) \quad \left(\frac{dr}{d\lambda}\right)^2 = \frac{1}{\ell^2} - W^2(r)$$

$$(5.11) \quad \frac{d\phi}{d\lambda} = \frac{\ell}{r^2}$$

$$(5.12) \quad \frac{dt}{d\lambda} = \frac{1}{\ell r^2 W^2(r)}$$

$$(5.13) \quad \frac{d\theta}{d\lambda} = 0$$

$$\text{where (5.14)} \quad W^2(r) \equiv \frac{1}{r^2} \left(1 - \frac{2M}{r} + \frac{Q^2}{r^2}\right)$$

λ is an affine parameter and ℓ is the impact parameter defined as the ratio p_ϕ/p_t (i.e. L/E). From (5.10) we see that the allowed region for the motion of photons is characterized by

$$(5.15) \quad \frac{1}{\ell^2} \geq W^2(r)$$

The curves of $W^2(r)$ in various cases are shown in Figure 5.3.

First, we consider the $\frac{Q}{M} < 1$ case which is shown in Figure 5.3(a). For this case, we are interested in the final optical behavior of a collapsing star. Those photons reaching the distant observer at the latest stage must have had a nearly vanishing radial velocity during the propagation. This nearly vanishing velocity may happen in two cases. First case is that the photon was emitted at $R_+ < r < r_c$ with

an impact parameter $l \leq l_c$ thus its radial velocity would have been nearly zero when it passed through $r \approx r_c$. Second case is that the photon was emitted at $r \geq R_+$ where $W^2(r) \approx 0$, thus its radial coordinate velocity would have been nearly zero due to the infinite time dilatation there. It is these photons which contribute the latest luminosity of a star collapsing towards the event horizon.

Then we consider the $\frac{Q}{M} > 1$ cases which are shown in Figure 5.3(b). For these cases, the behaviors of $W^2(r)$ are slightly different as Q/M is larger or less than $\frac{3}{2\sqrt{2}}$. It is monotonically decreasing from infinity to zero for $\frac{Q}{M} > \frac{3}{2\sqrt{2}}$, instead, it has a kink during the decreasing for $\frac{Q}{M} < \frac{3}{2\sqrt{2}}$ (see Figure 5.3(b1)). r_{\max} is located in the range between $2M$ (if $Q/M \approx 1$) and $3M/2$ (if $Q/M \approx \frac{3}{2\sqrt{2}}$) and r_{\min} is located in the range between M (if $Q/M \approx 1$) and $3M/2$ (if $Q/M \approx \frac{3}{2\sqrt{2}}$). Here the most relevant feature for our purpose is that both $W^2(r)$ and $r^2 W^2(r)$ tend to infinity when r tends to zero. It implies that a photon emitted at the later time would have a smaller radial coordinate velocity and a smaller impact parameter l . This character determines the latest optical behavior of a star collapsing towards the singularity at $R=0$.

5.4 Optical Appearance of a Continuously Collapsing Charged Star

After knowing the motion of the collapsing stellar surface and the photons emitted by it, we are confronted with the problem of investigating the propagation of photon flow in order to know the optical appearance of this collapsing star from the viewpoint of a distant observer. It was Podurets⁴ who first introduced the concept of phase space and the Liouville theorem into this problem, and found out the luminosity of a uncharged non-rotating collapsing star is decreasing exponentially with a time constant $3\sqrt{3}M$ [†]. Soon after, Ames and Thorne⁵ studied this problem by using the same method, but with much greater details. Now we are in the position to apply this technique to a collapsing charged star.

The basic idea of this technique lies in the fact that the photon number density N in the phase space is conserved along the trajectory of the photon as ensured by the Liouville theorem. All observable quantities can be expressed through this density N .

[†] Podurets gave an incorrect time constant $3\sqrt{3}M/2$ due to an error in his computation. This correct result was actually obtained by Ames and Thorne.⁵

(5.16) The spectrum
$$F(\nu_o, t_o) = \int \nu_o^3 N d\Omega = \int \nu_o^3 N \frac{2\pi l dl}{r_o^2}$$

(5.17) The intensity distribution
$$I(l, t_o) = \int \nu_o^3 N d\nu_o$$

(5.18) The total flux
$$F(t_o) = \int I(l, t_o) d\Omega = \int F(\nu_o, t_o) d\nu_o$$

Here the foot index o means that the quantity takes the value at observed time and space and later on a foot index e will be used to show that the quantity takes the value at emitting time and space. By re-tracing the photons which is observed at time t_o to its emitting time t_e along its trajectory, the photon number density N can be related to those parameters which is characterizing the photon and its source at emitting time t_e and space R_e .

(5.19)
$$N = \frac{J}{2\pi \nu_e^2 n_\mu p^\mu} \delta\left(\frac{\partial t}{\partial \tau} p_o + \frac{\partial R}{\partial \tau} p_r + \nu_e\right)$$

where ν_e is the assumed monochromatic frequency of the radiation, the Planck constant h has been taken as unit, J is the brightness of the star, P_μ or P^μ is 4-momentum of the photon, n_μ is the unit vector normal to the hypersurface of the collapsing surface and $\frac{\partial x^\mu}{\partial \tau}$ is the 4-velocity of the collapsing stellar surface. Except J and ν_e which are considered as arbitrary parameters all other relevant quantities have already been studied in the last two sections. $\frac{\partial x^\mu}{\partial \tau} = \left(\frac{dt}{d\tau}, \frac{dR}{d\tau}, 0, 0\right)$ are given by (5.6) and (5.8). Suppose that the hypersurface of the collapsing stellar boundary is described by $F(R, t) = \text{Const.}$ and that

its normalized normal 4-vector is $n_\mu = (n_0, n_1, 0, 0)$. Then we have a relation between n_μ and $\frac{\partial x^\mu}{\partial \tau}$.

$$(5.20) \quad \frac{n_0}{n_1} = \frac{(\frac{\partial F}{\partial t})_R}{(\frac{\partial F}{\partial R})_t} = -(\frac{\partial R}{\partial t})_F = -\frac{(\frac{\partial R}{\partial t})_F}{(\frac{\partial t}{\partial \tau})_F}$$

where $(\frac{\partial R}{\partial t})_F$ and $(\frac{\partial t}{\partial \tau})_F$ are just the components of the 4-velocity of the surface mass element. Since n_μ is normalized, we get

$$(5.21) \quad \begin{aligned} n_0 &= -v_e \left[\frac{1 - \frac{2M}{R_e} + \frac{Q^2}{R_e^2}}{(1 - \frac{2M}{R_e} + \frac{Q^2}{R_e^2})^2 - v_e^2} \right]^{1/2} \\ n_1 &= \left[\frac{1 - \frac{2M}{R_e} + \frac{Q^2}{R_e^2}}{(1 - \frac{2M}{R_e} + \frac{Q^2}{R_e^2})^2 - v_e^2} \right]^{1/2} \end{aligned}$$

where $v_e \equiv \frac{\partial R}{\partial t_e}$ is the coordinate velocity of stellar surface. Then,

we still have to know the 4-momentum of the photon at the emitting

time t_e . The quantity which we actually need is P_i/P_o , since $P_o = \nu_o$

is the observed frequency at $r_o = \infty$.

$$(5.22) \quad \frac{P_i}{P_o} = \frac{g_{rr} \frac{dr}{d\lambda}}{g_{tt} \frac{dt}{d\lambda}} = - \left(1 - \frac{2M}{R_e} + \frac{Q^2}{R_e^2}\right)^{-1} \sqrt{1 - \frac{R^2}{R_e^2} \left(1 - \frac{2M}{R_e} + \frac{Q^2}{R_e^2}\right)}$$

Substituting all these quantities into (5.19), we rewrite the expression of N as follows.

$$(5.23) \quad N = \frac{J}{2\pi\nu_e^3} \frac{\Phi(l, t_o)}{\Psi(l, t_o)} \delta(\nu_o \Phi(l, t_o) - \nu_e)$$

where

$$(5.24) \quad \Psi(l, t_o) \equiv \frac{n_\mu p^\mu}{\nu_o} = \left[\frac{1 - \frac{2M}{R_e} + \frac{Q^2}{R_e^2}}{(1 - \frac{2M}{R_e} + \frac{Q^2}{R_e^2})^2 - v_e^2} \right]^{1/2} \cdot \left\{ -\frac{v_e}{1 - \frac{2M}{R_e} + \frac{Q^2}{R_e^2}} + \left[1 - \frac{R^2}{R_e^2} \left(1 - \frac{2M}{R_e} + \frac{Q^2}{R_e^2}\right) \right]^{1/2} \right\}$$

$$(5.25) \quad \Phi(l, t_o) = \frac{(1 - \frac{2M}{R_e} + \frac{Q^2}{R_e^2}) - v_e \left[1 - \frac{R^2}{R_e^2} \left(1 - \frac{2M}{R_e} + \frac{Q^2}{R_e^2}\right) \right]^{1/2}}{\left[(1 - \frac{2M}{R_e} + \frac{Q^2}{R_e^2})^2 - v_e^2 \right]^{1/2}} \cdot \frac{1}{(1 - \frac{2M}{R_e} + \frac{Q^2}{R_e^2})^{1/2}}$$

Then, the last step is to find the dependence of R_e on t_o . It derives

from two relations. The solution of the radial motion of a photon

(see (5.10) and (5.12)) gives us one relation.

$$(5.26) \quad t_0 = t_e + \int_{R_e}^{r_0} \frac{dr}{\left(1 - \frac{2M}{r} + \frac{Q^2}{r^2}\right) \sqrt{1 - \frac{Q^2}{r^2} \left(1 - \frac{2M}{r} + \frac{Q^2}{r^2}\right)}}$$

Another relation is the solution of the motion of the stellar surface (see (5.9)).

$$(5.27) \quad t_e = t_i - \int_{R_i}^{R_e} \frac{dR}{\left(1 - \frac{2M}{R} + \frac{Q^2}{R^2}\right) \sqrt{1 - \frac{1 - \frac{2M}{R} + \frac{Q^2}{R^2}}{\left(\tilde{\epsilon} - \frac{\tilde{\epsilon} Q}{R}\right)^2}}}$$

where t_i and R_i are the initial time and radius of stellar collapse respectively. Now all materials have been well prepared. Let us go on to study the optical appearance of two continuously collapsing cases. One case is collapsing towards the event horizon and another one case is collapsing towards the singularity.

a) Collapsing towards the event horizon ($Q/M \ll 1$ case).

For simplicity, we consider the intensity at the centre of its optical disc. The relevant photons are emitted at $R_e \approx R_+$ with $l \approx 0$. Then we can expand every formula to a power series of $R_e - R_+$ and keep the dominant term only. After the cumbersome calculations, the results come out as follows. First we find the final dynamical behavior of the star, as seen by a distant observer.

$$(5.28) \quad R_e - R_+ = A_1 e^{-t/T}$$

where $T \equiv \frac{R_+^2 + 2MR_+ - Q^2}{2\sqrt{M^2 - Q^2}}$ is a time constant determined by the star and

A_1 is another constant. The redshift of photons, as shown by the delta

function in (5.23), is determined by Φ , which is proved to be inversely proportional to $R_e - R_+$.

$$(5.29) \quad \frac{\nu_e}{\nu_o} \equiv 1+z = \Phi(l=0, t_o) = A_2 (R_e - R_+)^{-1} = A_2 \bar{A}_1 e^{t_o/T}$$

where A_2 is another constant. It says that the redshift tends to infinity with the same timescale. Finally we consider the intensity at the centre of the disc. $I(l=0, t_o)$ is proved to be proportional to $R_e - R_+$ by a power of 4.

$$(5.30) \quad I(l=0, t_o) = A_3 (R_e - R_+)^4 = A_3 \bar{A}_1^4 e^{-t_o/T}$$

where A_3 is another constant. It tells that the corresponding timescale is one fourth of T . The constants A_1 , A_2 and A_3 depend on the staller luminosity J and other details of the collapse. They are not interesting for us.

The timescale T is worthy to be given more explanation. From its definition we see that T increases monotonically with an increasing Q . When $Q=0$, T equals $4M$. It is just the well known result for a Schwarzschild black hole. Since $4M$ is a very short timescale, (by conventional unit, $4M=2 \cdot 10^{-5}$ sec, for $M=1M_\odot$), this phenomenon is impossible to be observed by today's technique. For the charged case, we see that T tends to infinity, when $Q \rightarrow M$. It implies that the timescale might be long enough to be observed, if a highly charged collapse

sing star does exist in nature.

The result of $T \rightarrow \infty$ means that the exponential term is no more the leading term for the $Q=M$ case; therefore the things should be reconsidered. For $Q=M$ case, the Reissner-Nordstrom metric reduces to

$$(5.31) \quad d\tilde{s}^2 = -\left(1 - \frac{M}{R}\right)^2 dt^2 + \left(1 - \frac{M}{R}\right)^{-2} dR^2 + R^2(d\theta^2 + \sin^2\theta d\varphi^2)$$

The location of the event horizon is $R=M$. After repeating all the procedures for this metric, we find that the power law works instead of the previous exponential behavior.

$$(5.32) \quad R_e - M = \left(\frac{t_0}{2M^2} + c\right)^{-1}$$

$$(5.33) \quad \frac{\nu_e}{\nu_0} \propto (R_e - M)^{-2} = \left(\frac{t_0}{2M^2} + c\right)^2$$

$$(5.34) \quad I(l=0, t) \propto (R_e - M)^8 = \left(\frac{t_0}{2M^2} + c\right)^8$$

where c is a constant which depends on many details.

b) Collapsing towards the singularity ($Q/M > 1$ case).

As it has been pointed out that even in $Q/M > 1$ case, collapsing towards the singularity happens only if $\tilde{\epsilon} < -1$. Now we consider this case and compare the results with those of the black hole case. We still concentrate ourself on the latest stage of collapse.

The dynamical behavior in this case is very different from that in the black hole case.

$$(5.35) \quad v \equiv \frac{dr}{dt} = \sqrt{\frac{\tilde{\epsilon}-1}{e^{\tilde{\epsilon}}}} \alpha^2 \frac{1}{R^2} + O\left(\frac{1}{R}\right)$$

The final velocity is infinite, instead of vanishing in the black hole case; thus the collapsing star takes finite time to reach the singularity. The redshift of photons emitted at the latest stage are different for $l=0$ and $l \neq 0$ cases. In fact, formula (5.25) gives

$$(5.36) \quad \begin{aligned} \frac{\nu_e}{\nu_o} &= \Phi \propto R \rightarrow 0 & \text{for } l=0 \\ \frac{\nu_e}{\nu_o} &= \Phi \propto R^{-1} \rightarrow \infty & \text{for } l \neq 0 \end{aligned}$$

We do not think the infinite blueshift can be seen, since it happens only when l is exactly zero, thus the corresponding phase volume is vanishing. The phenomenon we finally see is still an infinitely increasing redshift. Then consider the intensity. Just like the black hole case, I is proportional to R by a power of 4.

$$(5.37) \quad I(l=0, t_0) = \frac{5}{2\pi} \frac{1}{\Phi^3 \psi} \propto \Phi^{-4} \propto R^4 \rightarrow 0$$

This means that the singularity is also black. Anyhow, the detailed behavior of $R \rightarrow 0$ is very different from the corresponding behavior of $R - R_+ \rightarrow 0$ in the black hole case. Therefore, if how the collapsing object fades away could be observed, we would find that the singularity is not so black as a black hole! These appearances of a collapsing overcharged star ($Q > M$) are very similar to those of a collapsing overrapidly rotating star ($a > M$), that have been studied by de Felice⁴.

There is one point more which is worthy to be emphasized here. In order to have a continuous collapse, the specific charge \tilde{e} at the surface must be less than -1 . This means that a positively charged star should have a negatively charged surface, and this peculiar charge distribution should be maintained as long as its radius tends to zero. It is quite inconceivable. Therefore, it might suggest that the formation of a charged naked singularity by collapsing is in fact impossible. Moreover, several years ago Cohen and Gaultreau⁶ showed that it is impossible to form a charged naked singularity by injecting overcharged matter into a black hole. Consequently, we are probably forced to reach a negative answer, that is to say, a charged naked singularity is completely out of reality, in agree with the Cosmic censorship hypothesis.

5.5 Vibrating Charged Stars

If an overcharged star ($Q > M$) can exist in nature, its surface should probably be charged with the same sign. Figure 5.2(b) shows that in this case, once the star collapses, the collapse will be stopped by the repulsive core. Then it leads to the formation of a vibrating star. In this section, we consider its optical appearance. For the sake of simplicity, we set $\tilde{\epsilon} = 0$.

Let us first neglect radiations, thermal processes etc. during the vibration, so that the specific energy \tilde{E} should be constant. Setting $\tilde{E} = V(R)$ (see (5.7)), we find out the vibrating interval as extending from R_- to R_+ , where

$$(5.38) \quad R_{\pm} = \frac{M \pm \sqrt{M^2 - Q^2(1 - \tilde{E}^2)}}{1 - \tilde{E}^2}$$

One of the extreme cases is $\tilde{E} = 1$, the vibration proceeds from infinity to $\frac{Q^2}{2M}$, and another extreme case is $\tilde{E} \approx \sqrt{1 - \frac{M^2}{Q^2}}$, the star vibrates near the equilibrium position $R = Q^2/M$. Proper time period of vibration can be got from (5.6) by integration.

$$(5.39) \quad \tau = 2 \int_{R_-}^{R_+} \frac{dR}{\sqrt{-(1 - \tilde{E}^2) + \frac{2M}{R} + \frac{Q^2}{R^2}}} = \frac{2\pi M}{(1 - \tilde{E}^2)^{3/2}}.$$

Although period τ can be arbitrary large as if $\tilde{E}^2 \approx 1$, in a reasonable case τ must be of the same order as $2\pi M$, since the initial configuration would not be so unstable. $2\pi M$ is actually a very short time

(about 10^{-4} sec). When a star vibrates so rapid, its vibrating energy will be dissipated soon by several possible mechanisms. Therefore a small vibrating configuration is in fact more probable. For these configurations, the specific energy \tilde{E} is nearly equal to $\sqrt{1 - \frac{M^2}{Q^2}}$ and the vibrating period is about $\frac{2\pi Q^3}{M^2}$. For dealing with its appearance, the coordinate time period is more relevant. Noting that $\frac{dt}{d\tau} = \frac{\tilde{E}}{1 - \frac{2M}{R} + \frac{Q^2}{R^2}}$ and $R \approx \frac{Q^2}{M}$, the average factor of time dilatation is $\frac{1}{\tilde{E}}$. Therefore the observed period reads

$$(5.40) \quad T = \frac{2\pi Q^3}{\tilde{E} M^2} = \frac{2\pi Q^3}{M^2 \sqrt{1 - \frac{M^2}{Q^2}}}$$

It depends on $\frac{M^2}{Q^2}$ sensitively when M/Q is nearly 1.

Then we turn our attention to its optical phenomenon. The redshift of the photons emitted by a vibrating charged star is described by $\phi(l, R_e)$ expressed in (5.25). In this case, v_e appearing in (5.25) is $\pm \frac{1 - \frac{2M}{R_e} + \frac{Q^2}{R_e^2}}{\tilde{E}} \sqrt{\tilde{E}^2 - 1 + \frac{2M}{R_e} + \frac{Q^2}{R_e^2}}$ (see (5.9)). The dependence of ϕ on R_e is shown in Figure 5.4. For the photon with $l=0$, $\phi(R)$ changes from $1/\tilde{E}$ to ϕ_{\max} then decreases to $1/\tilde{E}$ when the star shrinks. During another half period, $\phi(R)$ decreases from $1/\tilde{E}$ to ϕ_{\min} , then increases to $1/\tilde{E}$. ϕ_{\max} and ϕ_{\min} read as

$$(5.41) \quad \phi_{\max} = \phi\left(\frac{Q^2}{M}\right) = \frac{\tilde{E} + \sqrt{\tilde{E}^2 - (1 - \frac{M^2}{Q^2})}}{1 - \frac{M^2}{Q^2}} \quad \text{for } v < 0$$

$$(5.42) \quad \phi_{\min} = \phi\left(\frac{Q^2}{M}\right) = \frac{\tilde{E} - \sqrt{\tilde{E}^2 - (1 - \frac{M^2}{Q^2})}}{1 - \frac{M^2}{Q^2}} \quad \text{for } v > 0$$

respectively. For other values of l , the locus is confined to the interior of the locus for $l=0$. By other words, Photons with $l=0$

Have the maximum frequency shift during one period. The maximum shift is

$$(5.43) \quad \frac{\Delta \nu_0}{\nu_0} = \frac{1}{\phi_{\min}} - \frac{1}{\phi_{\max}} = 2 \sqrt{\tilde{E}^2 - (1 - \frac{M^2}{Q^2})}$$

For the small vibration case, it is a small quantity since \tilde{E} is slightly larger than $\sqrt{1 - \frac{M^2}{Q^2}}$. In fact the phenomenon what we see is an almost steady redshift.

$$(5.44) \quad \frac{\nu_e}{\nu_0} = \phi \approx \phi_{\max} \approx \phi_{\min} \approx \frac{1}{\sqrt{1 - \frac{M^2}{Q^2}}}$$

When M/Q is very close to 1, the redshift is very large. Therefore it could be confused with the redshift induced from other sources, for example, the recession redshift of a distant galaxy.

5.6 Conclusions

We summarize the conclusions drawn in this chapter as follows.

a) The optical phenomenon of the collapse of a mildly charged star ($Q \leq M$) is qualitatively the same as that of an uncharged star. Mainly we mean an infinitely increasing redshift and an asymptotically vanishing luminosity. However, the timescale is larger with a larger Q . If there is a star with Q less than but nearly equal to M , the timescale for optical observation of the collapse might be long enough to be detected.

b) The characterised feature of the collapse of an overcharged star ($Q > M$) is gravitational vibration. The timescale is even shorter than that of the collapse of an uncharged star. After the vibration has been damped out, a new stable configuration with a radius $R = \frac{Q^2}{M}$ can be formed. If Q is larger than but nearly equal to M , optically we can see a large enough redshift from this stable configuration or from its small vibrating state.

c) If the charge distribution in an overcharged star can be peculiar enough to ensure a negatively charged surface ($\tilde{e} < 1$), it can collapse towards the naked singularity. The optical appearance of collapsing towards the singularity is very similar to that of

collapsing towards the event horizon. The difference exists in the details. If it can be proved that such a peculiar distribution cannot happen, we conclude that a non-rotating charged naked singularity is an object out of reality.

References for Chapter V

- 1) M Calvani, F de Felice and L Nobili; (1978) Nuovo Cim Lett 23, 539.
- 2) H Reissner; (1916) Ann Phys (Germany) 50, 106.
- 3) G Nordstrom; (1918) Proc Kon Ned Akad Wet 20, 1238.
- 4) M A Podurets; (1964) *Astr Zh* 41, 1090. (Soviet Astr 8, 868 (1965))
- 5) W L Ames and K S Thorne; (1968) Ap J 151, 659.
- 6) J M Cohen and R Gautreau; (1979) Phys Rev D19, 2273.

MAIN CONCLUSIONS

In this thesis, some aspect of the fate of collapsing stellar cores have been studied. Detailed conclusions have been represented in the appropriate sections of each chapter. Here we emphasize some interesting points emerged from our main results.

In the study of collapsing rotating cores, the most interesting result is that a newly formed neutron star should be a fast rotator having a value of ratio a/m of the order of one, despite of the fact that observed neutron stars all have ^{very} small values of a/m (of the order of 10^{-2} to 10^{-4}). We have found four evidences or relevant facts in supporting such a conclusion.

a) The large proper velocities of neutron stars may be transformed from their rotational energy^{ies}. If the mechanism is that shown by Harrison and Tademaru, the evaluated value of ratio a/m of a newly formed neutron star is of the order of 1 (see Chapter II).

b) In the study of the gravitational radiation of a collapsing core we see that in forming a neutron star, the final value of ratio a/m does not depend sensitively on the initial a/m . We find that the final value of ratio a/m is about 1, if the initial a/m is in the range of 1 to 10 (see Chapter III).

c) As an observational fact, the value of ratio a/m of a main-sequence stellar core is in the range of 10 to 100. By considering all known mechanisms, we cannot find any way to reduce it to the value of 10^{-2} or even much less in forming a neutron star (see Chapter II).

d) From the Newtonian argument and also relativistic models we find that the upper limit of ratio a/m which can be sustained by a rotating stable configuration is about 1 (see Chapter II).

A noticeable implication emerges. For the cases in which the mass of a collapsing object is larger than the limiting mass of a neutron star, the study of the final state other than the black hole due to fast rotation is not only an interesting problem but also a realistic task.

In the study of collapsing charged stellar cores, our main results are the following two (see Chapter V).

a) If overcharged stars or stellar cores do exist in nature, its collapse would probably lead to form a vibrating dense star rather than a naked singularity. This result is in supporting the hypothesis of cosmic censorship.

b) Optically, we will see a quasi-stationary redshift from these

objects. Specially, the redshift can be large enough to confuse with a cosmological redshift of a distant galaxy, if charge Q is nearly equal to its mass m .

The influence of neutrinos to the collapsing process has also been studied. The problem is limited to the neutrino trapping by the strong gravitational field in dense objects, and the corresponding results are as follows (see Chapter IV).

The gravitational trapping effect of neutrinos is considerably increased, if the neutrino has a rest mass. However, if massive neutrinos are trapped only by the gravitational field, the effect would not be strong enough to influence significantly an object as dense as a neutron star. Nevertheless, as the behavior of collapsing objects appears to be very sensitive to the neutrino concentration, even a weak contribution to the neutrino opacity by the gravitational field may be significant and worthy to be considered in a more detailed investigation.

ACKNOWLEDGEMENT

I would like to express my heartfelt thanks to my supervisor Prof. F. de Felice for his introducing into this interesting field and also for his helpful instruction. Dr. J. Miller is much acknowledged for his several enlightening discussions in Oxford and in Trieste.

I appreciate very much to Prof. N. Dallaporta and Prof. B. Cester for their invaluable encouragement during the course of the work.

Thanks are also given to Dr. C. Bordari for his kindness in correcting my grammatical mistakes.

Table 1.1 Nuclear Burning Stages of a $25M_{\odot}$ Star

Burning stage	Temperature(K)	Density (gcm^{-3})	Timescale (yr)
H	$4 \cdot 10^7$	4	$7 \cdot 10^6$
He	$2 \cdot 10^8$	$6 \cdot 10^2$	$5 \cdot 10^5$
C	$7 \cdot 10^8$	$6 \cdot 10^5$	$5 \cdot 10^2$
Ne	$1.5 \cdot 10^9$	$4 \cdot 10^6$	1
O	$2 \cdot 10^9$	$1 \cdot 10^7$	$5 \cdot 10^{-1}$
Si	$3.5 \cdot 10^9$	$1 \cdot 10^8$	$3 \cdot 10^{-3}$
pre-collapsing	$8 \cdot 10^9$	$3 \cdot 10^9$	

Table 2.1 Ratios a/m of 105 Neutron Stars

$Star$	P (sec)	\dot{P} (ns.d ⁻¹)	$a/m \cdot 10^3$	P/\dot{P} (10 ⁶ yrs)
0031+07	0.943	0.0359	0.60	36
0105+65	1.284	1.074	0.44	1.6
0138+59	1.223	0.015	0.46	110
0153+61	2.352	16.358	0.24	0.2
0254-54	0.448		1.3	
0301+19	1.386	0.103	0.41	18
0329+54	0.715	0.177	0.79	5.5
0355+54	0.156	0.379	3.6	5.6
0450-18	0.549	0.360	1.0	2.1
0525+21	3.745	3.462	0.15	1.5
0531+21	0.033	36.526	17	0.00124
0540+23	0.246	1.334	2.3	0.25
0611+22	0.335	5.161	1.7	0.089
0628-28	1.224	0.217	0.46	7.7
0736-40	0.375	0.086	1.5	6.0
0740-28	0.167	1.453	3.4	0.16
0809+74	1.292	0.014	0.44	130
0818-13	1.238	0.182	0.46	9.3
0823+26	0.531	0.145	1.1	5.0
0835-45	0.089	10.823	6.3	0.0113
0834+06	1.274	0.587	0.44	3.0
0835-41	0.767		0.74	
0904+77	1.579		0.36	
0940-55	0.664		0.85	
0943+10	1.098	0.305	0.51	4.9
0950+08	0.253	0.020	2.2	17
0959-54	1.437		0.39	
1055-51	0.197		2.9	
1112+50	1.656	0.224	0.34	10
1133+16	1.188	0.323	0.48	5.0
1154-62	0.401		1.4	
1221-63	0.216		2.6	
1237+25	1.382	0.083	0.41	23
1240-64	0.389		1.5	

Star	P (sec)	\dot{P} (ns.d ⁻¹)	$a_m \cdot 10^3$	P/\dot{P} (10 ⁶ yrs)
1323-62	0.532		1.1	
1354-62	0.456		1.2	
1359-50	0.690		0.81	
1426-66	0.787		0.72	
1449-65	0.180		3.1	
1451-68	0.263	0.259	2.1	1.4
1508+55	0.740	0.435	0.76	2.3
1530-53	1.369		0.41	
1541+09	0.748	0.038	0.76	27
1556-44	0.257		2.2	
1557-50	0.193		2.9	
1558-50	0.864		0.65	
1601-52	0.658		0.86	
1604-00	0.422	0.026	1.3	22
1641-45	0.455		1.2	
1642-03	0.388	0.154	1.5	3.5
1700-32	1.212	0.059	0.47	28
1700-18	0.802		0.70	
1706-16	0.653	0.550	0.87	1.6
1717-29	0.620		0.91	
1718-32	0.477	0.065	1.2	10
1727-47	0.830		0.68	
1730-22	0.872	0.002	0.65	600
1742-30	0.367	0.921	1.5	0.55
1747-46	0.742	6.040	0.76	0.17
1749-28	0.563	0.711	1.0	1.1
1813-26	0.593	0.001	0.95	810
1818-04	0.598	0.546	0.95	51
1819-22	1.874	0.050	0.30	0.23
1822-09	0.769	4.512	0.73	0.87
1826-17	0.307	0.483	1.8	0.26
1831-03	0.687	3.582	0.82	44
1831-04	0.290	0.009	2.0	2.0
1845-01	0.659	0.453	0.86	0.18
1845-04	0.598	4.480	0.95	0.50
1846-06	1.451	3.949	0.39	60

ϵ_{ran}	P (sec)	\dot{P} (ns·d ⁻¹)	$a_{\text{m}} \cdot 10^3$	$P_{\text{zp}} (10^6 \text{ yrs})$
1857-26	0.612	0.014	0.92	1.4
1858+03	0.655	0.646	0.86	2.0
1900-06	0.432	0.298	1.3	2.7
1900+01	0.729	0.356	0.78	2.8
1906+00	1.017	0.467	0.56	3.0
1907+02	0.495	0.248	1.1	2.7
1907+10	0.284	0.232	2.0	1.7
1910+20	2.233	0.825	0.25	3.7
1911-04	0.826	0.351	0.68	3.2
1915+13	0.195	0.621	2.9	0.43
1917+00	1.272	0.645	0.44	2.7
1918+19	0.821	0.065	0.69	17
1919+21	1.337	0.116	0.42	16
1920+10	1.078	0.706	0.52	2.1
1929+10	0.227	0.100	2.5	3.1
1933+16	0.359	0.519	1.6	0.95
1944+17	0.441	0.002	1.3	300
1946+35	0.717	0.607	0.79	1.6
1953+29	0.427	0.003	1.3	190
2002+30	2.111	6.416	0.27	0.45
2016+28	0.558	0.013	1.0	59
2020+28	0.343	0.160	1.6	2.9
2021+51	0.529	0.264	1.1	2.7
2045-16	1.962	0.947	0.29	2.8
2106+44	0.414	0.005	1.4	110
2111+46	1.015	0.062	0.56	22
2148+63	0.380	0.014	1.5	37
2154+40	1.525	0.283	0.37	7.4
2217+47	0.538	0.239	1.1	3.1
2223+65	0.683	0.825	0.83	1.1
2255+58	0.368	0.497	1.5	1.0
2303+30	1.576	0.251	0.36	8.6
2305+55	0.475	0.006	1.2	110
2319+60	2.256	0.588	0.25	5.3
2324+60	0.234	0.031	2.4	10

Table 2.2 The Values of a/m for Main-sequence Stars

M (M_{\odot})	R (10^5 km)	$V \sin i$ (km s^{-1})	a (km)	m (km)	a/m
1.0	7.0	10	12	1.5	7.9
1.1	7.8	29	38	1.7	22.4
1.2	8.3	90	127	1.8	70.6
1.3	8.9	126	190	2.0	95
1.4	9.5	148	238	2.1	113
1.5	10.0	161	274	2.3	119
1.7	11.0	183	343	2.6	132
1.9	11.9	197	399	2.9	138
2.1	12.3	204	427	3.2	133
2.3	13.7	231	537	3.5	153
2.5	14.5	270	665	3.8	175
2.7	15.3	280	727	4.1	177
3.0	16.5	306	857	4.5	194
3.3	17.6	320	956	5.0	191
3.8	19.2	333	1086	5.7	191
4.3	20.6	365	1277	6.5	196
4.8	22.0	377	1408	7.2	196
5.5	23.6	387	1551	8.3	187
6.3	25.4	395	1704	9.5	179
7.7	28.8	395	1932	11.6	167
10.0	32.1	400	2181	14.0	156

Table 2.3 The Values of a/m for a $1M_{\odot}$ Core
of the $10M_{\odot}$ Main-sequence Star
in the Rigidly Rotating Model

$\rho_{core} (gcm^{-3})$	$\omega (sec^{-1})$	a/m
0.15	$(0.6-1.2) \cdot 10^{-4}$	117-234
3	$(0.6-1.2) \cdot 10^{-4}$	16-32
7.8	$(0.6-1.2) \cdot 10^{-4}$	8.5-17

TABLE 2.4

The values of $\frac{a}{m}$ for 1 M_{\odot} core of a main sequence star in differentially rotating model

	I	II	III	IV	V
Angular momentum distribution law	$\Omega = \text{const}$	$j(\mu) = \frac{5J}{2M} [1 - (1-\mu)^{2/3}]$	same as II	same as II	$j(\mu) = \frac{J}{M} 2\mu$
Total angular momentum	3.17×10^{52}	3.17×10^{52}	1.12×10^{53}	5.7×10^{53}	5.01×10^{53}
Total mass	$15 M_{\odot}$	$15 M_{\odot}$	$15 M_{\odot}$	$30 M_{\odot}$	$30 M_{\odot}$
Equatorial velocity V_e	4.12×10^7	0.75×10^7	2.56×10^7	4.22×10^7	3.47×10^7
Equatorial radius R_e	4.10×10^{11}	3.56×10^{11}	3.73×10^{11}	5.74×10^{11}	4.90×10^{11}
Equatorial angular velocity	1.0×10^{-4}	2.1×10^{-5}	6.9×10^{-5}	7.4×10^{-5}	7.1×10^{-5}
Central angular velocity	1.0×10^{-4}	1.7×10^{-4}	5.8×10^{-4}	5.8×10^{-4}	5.9×10^{-4}
Central density ρ_c	5.2	5.2	6.8	4.7	4.2
Re/Rp	1.12	1.06	1.76	2.69	1.41
$\frac{a}{m}$	18.3	31.2	88.9	114	125

c.g.s. units are used.

Table 2.5 Evolution of the Ratio a/m

Period	Range of a/m or main mechanisms of a/m loss	A possible scenario
Main-sequence	$a/m = 10 - 100$	$a/m = 10 - 20$
Post main-sequence	Convection and circulation Magnetic field	Reduce to 5-10 by convection and circulation
Collapse	Neutrino emission Gravitational radiation	Reduce to 1 by gravitational radiation
Neutron star evolution	Rotation to translation Rotation to pulsating radiation	Reduce to 10^{-2} by converting for translation
Observed neutron stars	$a/m = 10^{-2} - 10^{-4}$	Due to pulsating radiation $a/m \approx 10^{-2}$ for young pulsars $a/m \approx 10^{-3} - 10^{-4}$ for old pulsars

Table 2.6 Critical Values of a/m in Relativistic
Models of Rotating Bodies

γ_s	0.3	0.5	0.62	From Fig. [†] 1.
e_{shed}	0.90	0.79	0.64	From Fig. [†] 1.
Ω^2/ϵ	1.4^2	1.6^2	1.7^2	From Tab. [†] 1-3.
$I \epsilon^{3/2}$	$3.81 \cdot 10^3$	$9.82 \cdot 10^3$	$1.39 \cdot 10^2$	From Tab. [†] 1-3.
$\gamma_s^*/2m$	1.961	1.333	1.169	From Formula (2.20).
a/m	1.35	1.25	1.26	From Formula (2.21).

† The daggered figures and tables are of the Butterworth and
Ipser's paper.

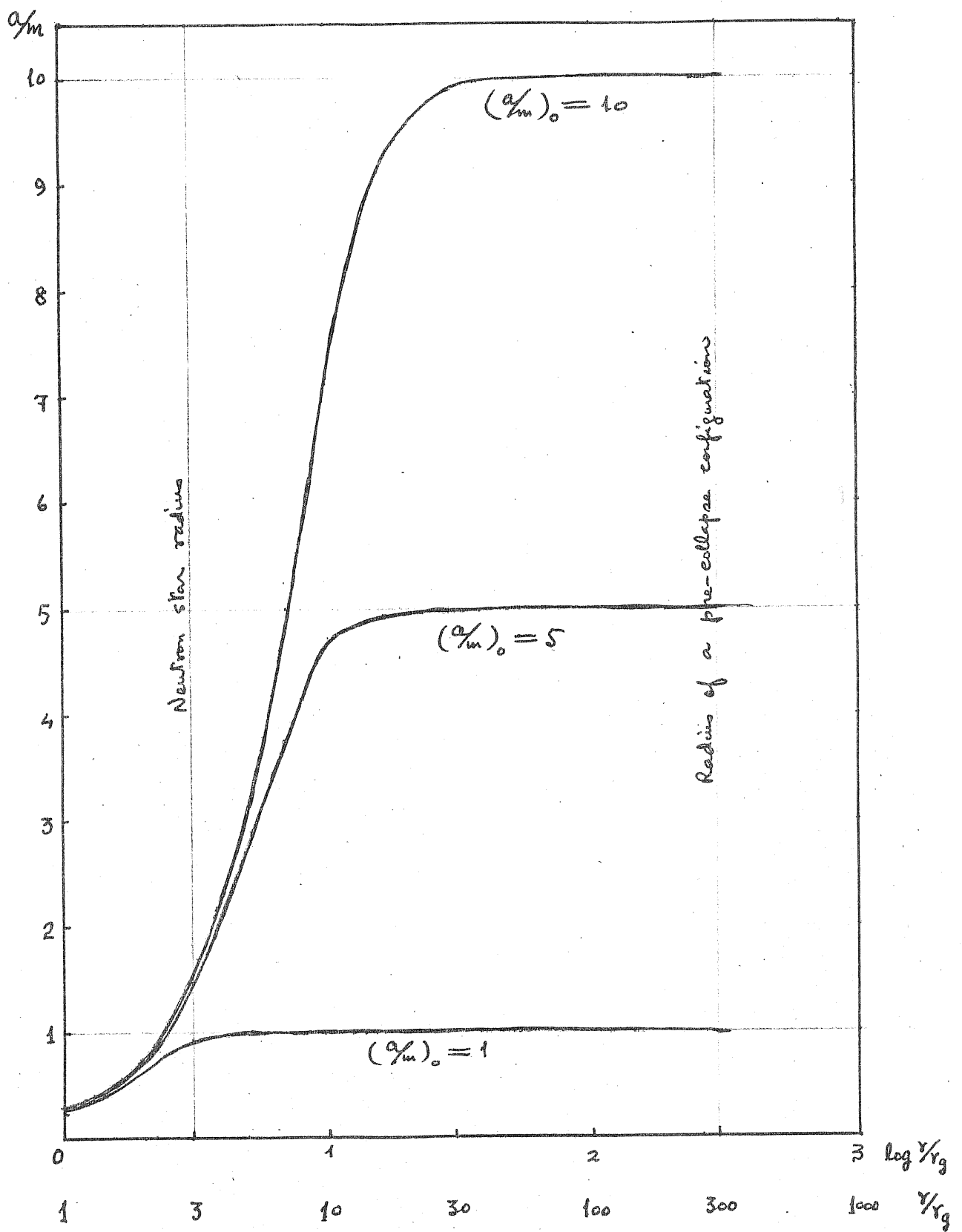


Figure 3.1 Solutions of Equation (3.16)

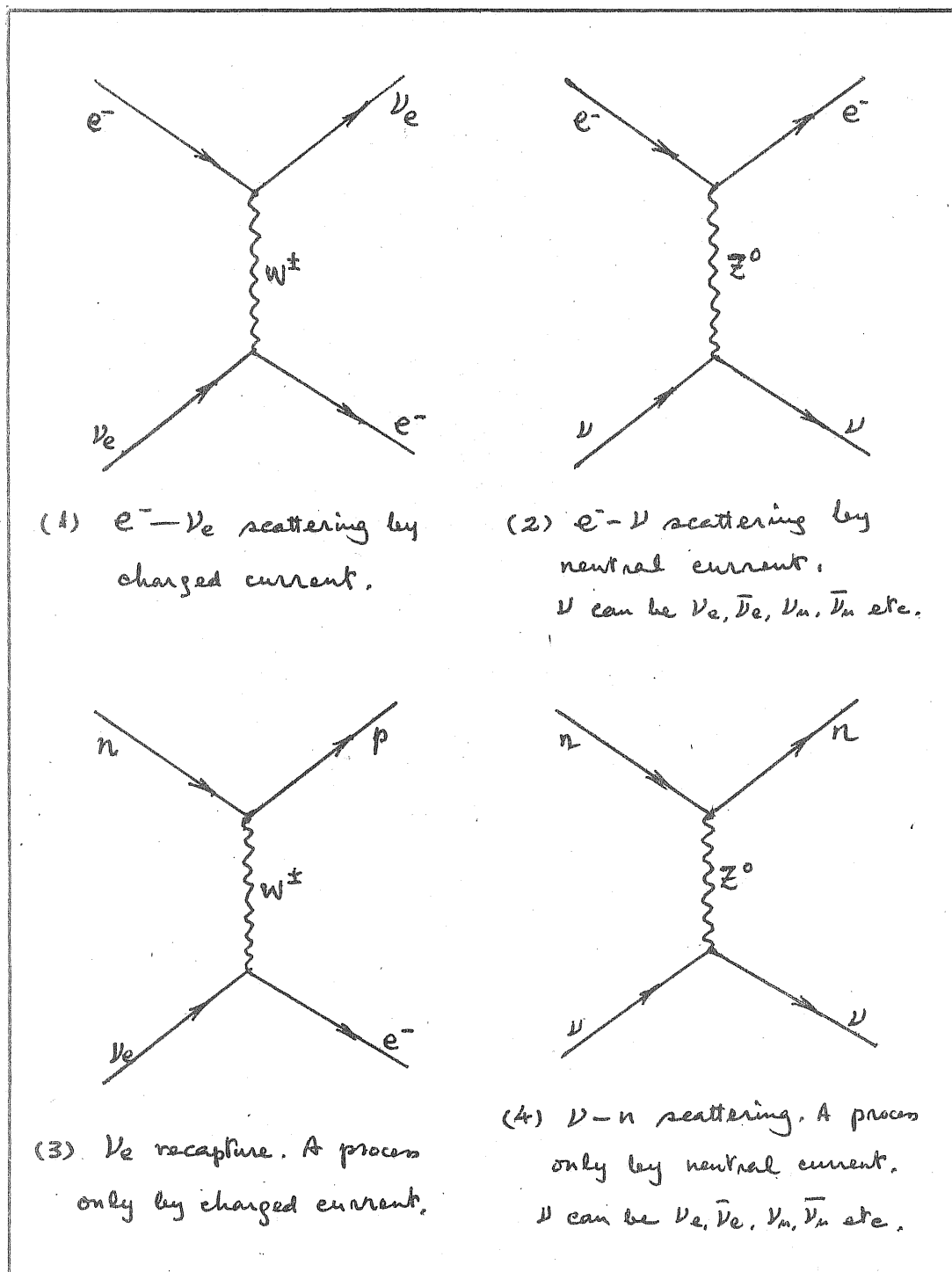


Figure 4.1 Main Mechanisms for Neutrino Opacity

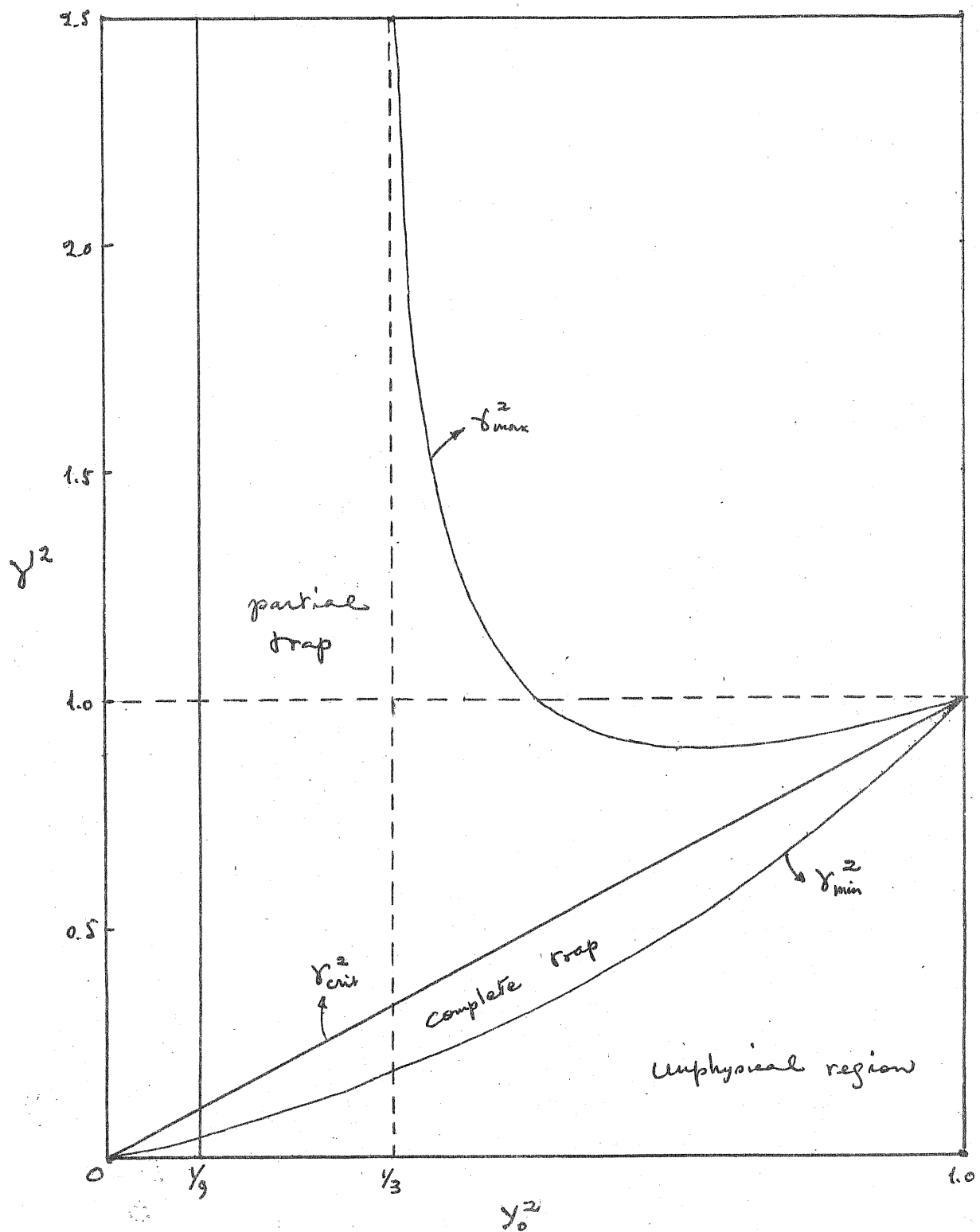


Figure 4.2 The Extent of Energy for Neutrino Trapping inside the star.

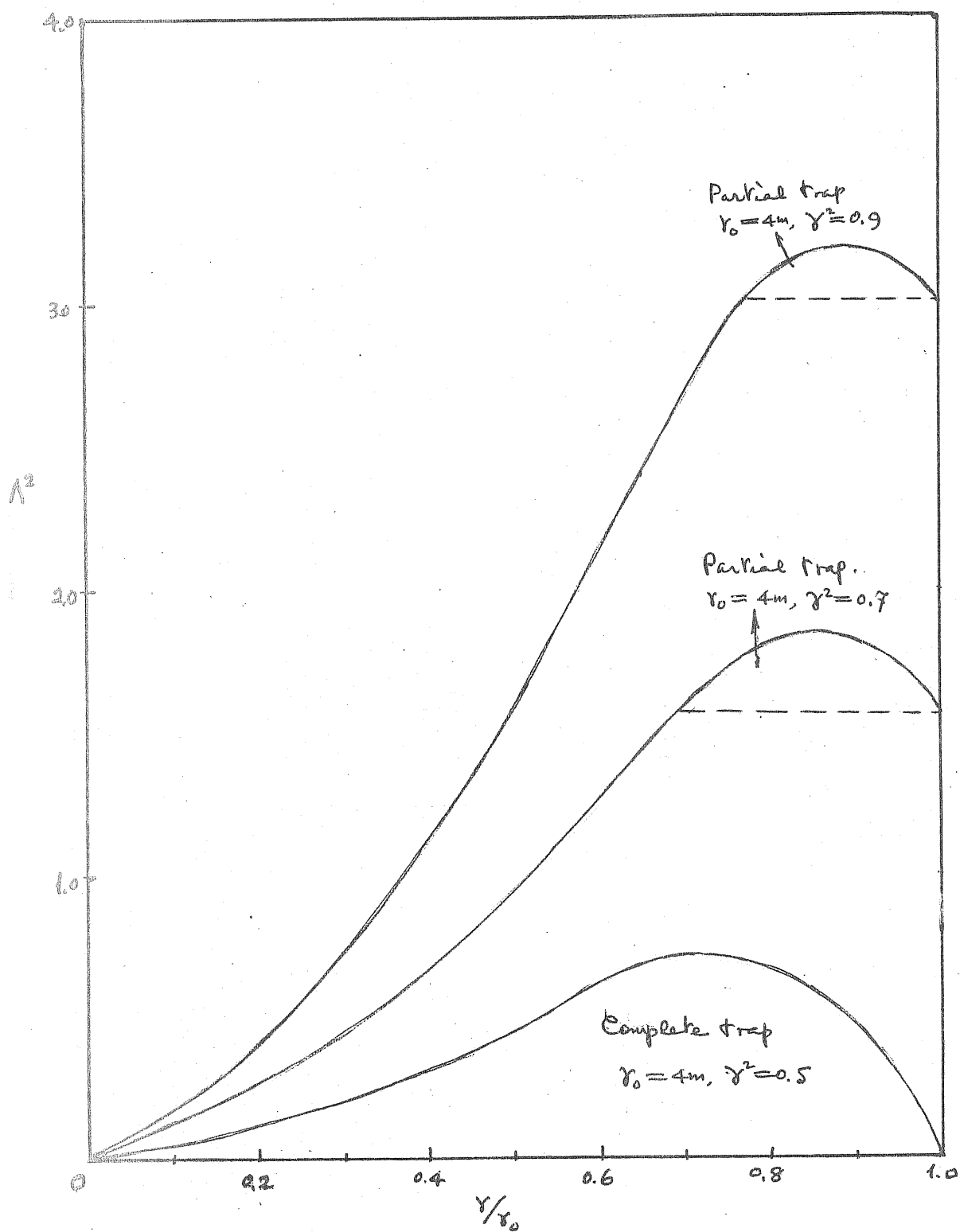


Figure 4.3 The shape of Traps in $A^2 - \gamma$ Plane

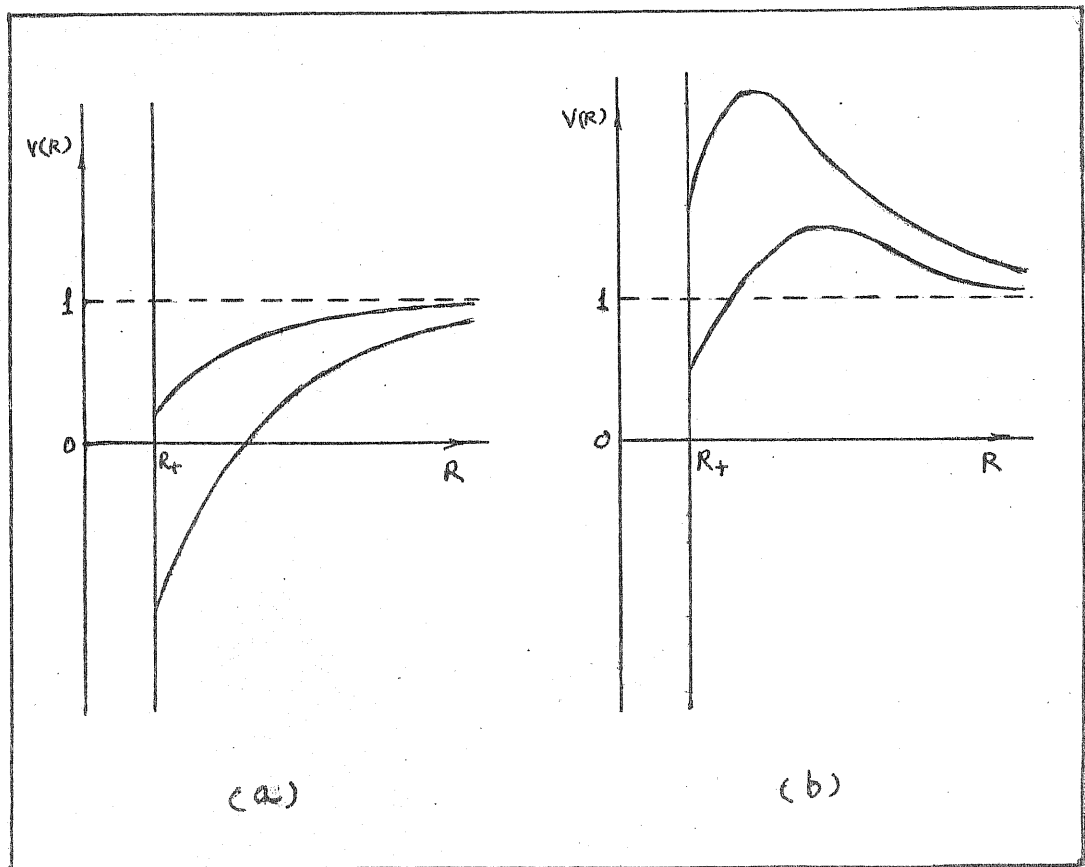


Figure 5.1 Potential Curves for the $Q_M < 1$ Cases.

(a) $\tilde{e} < \frac{M}{Q}$, no maximum, force is always attractive

(b) $\tilde{e} > \frac{M}{Q}$, force is attractive for $R_+ < R < R_{\max}$
force is repulsive for $R > R_{\max}$

where $R_{\max} = \frac{Q^2}{M - \sqrt{\frac{\tilde{e}^2}{\tilde{e}^2 - 1} (M^2 - Q^2)}}$ and

$$R_+ = M + \sqrt{M^2 - Q^2}$$

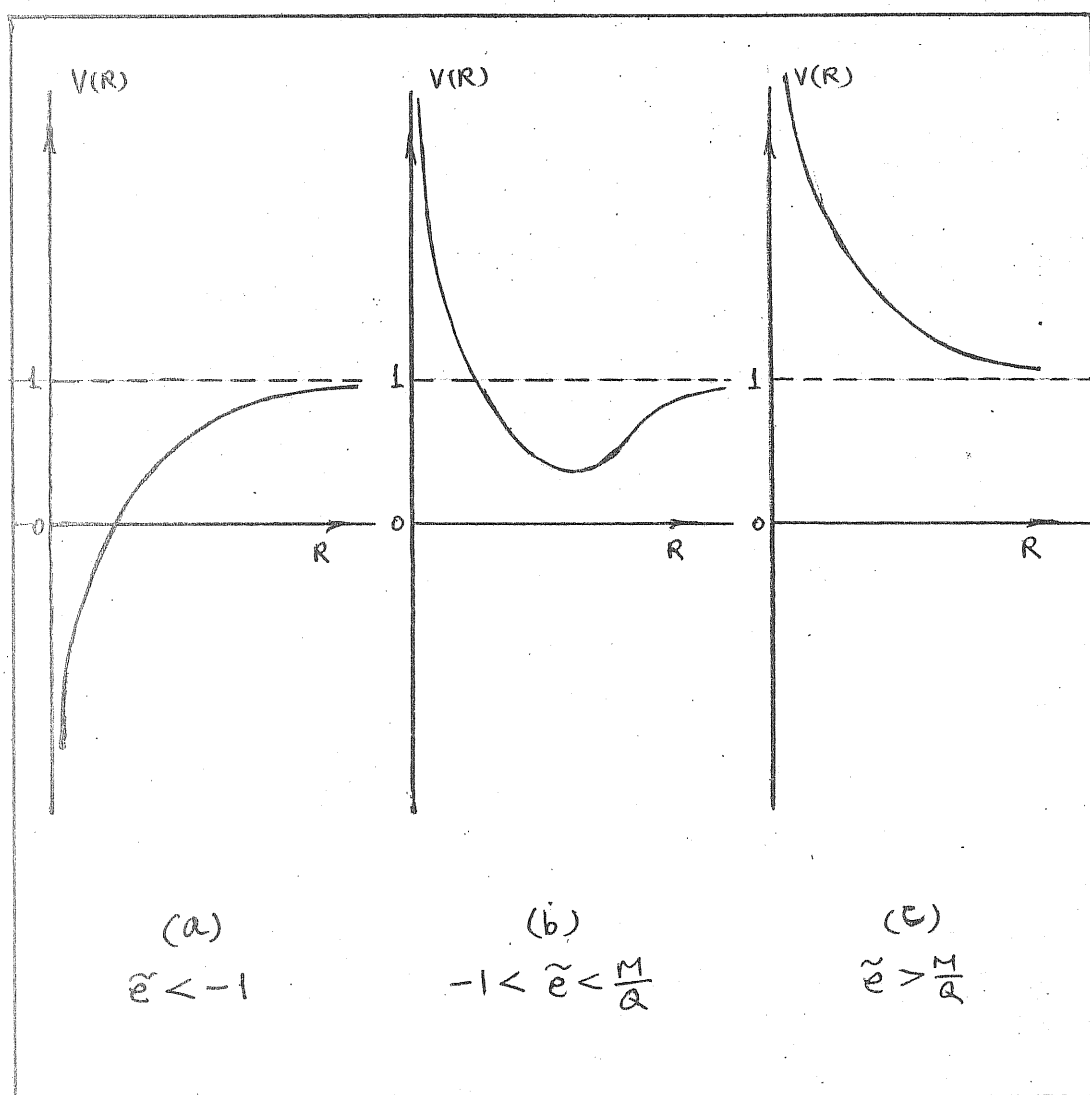
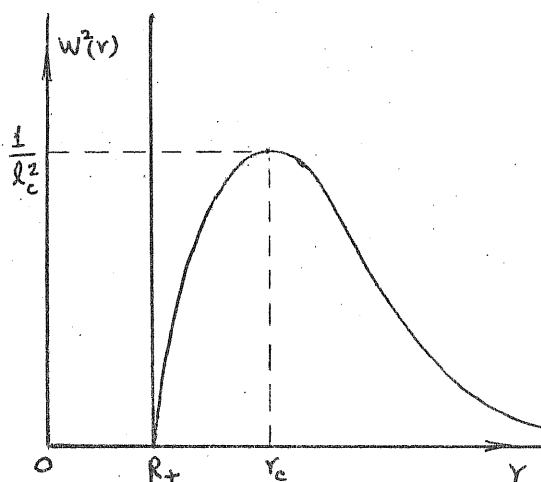
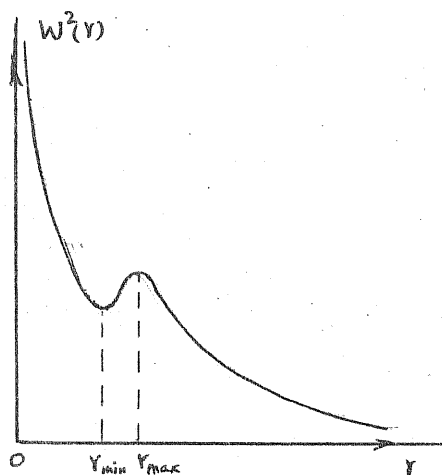


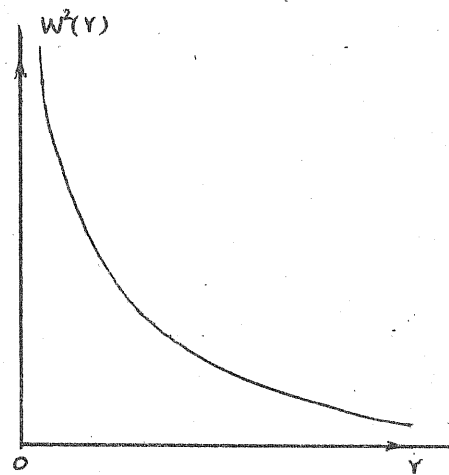
Figure 5.2 Potential curves for the $\frac{Q}{M} > 1$ Cases.



(a) $\frac{Q}{M} < 1$ case.



(b1) $\frac{3}{2\sqrt{2}} > \frac{Q}{M} > 1$ case.



(b2) $\frac{Q}{M} > \frac{3}{2\sqrt{2}}$ case.

Figure 5.3 Barrier for Photons

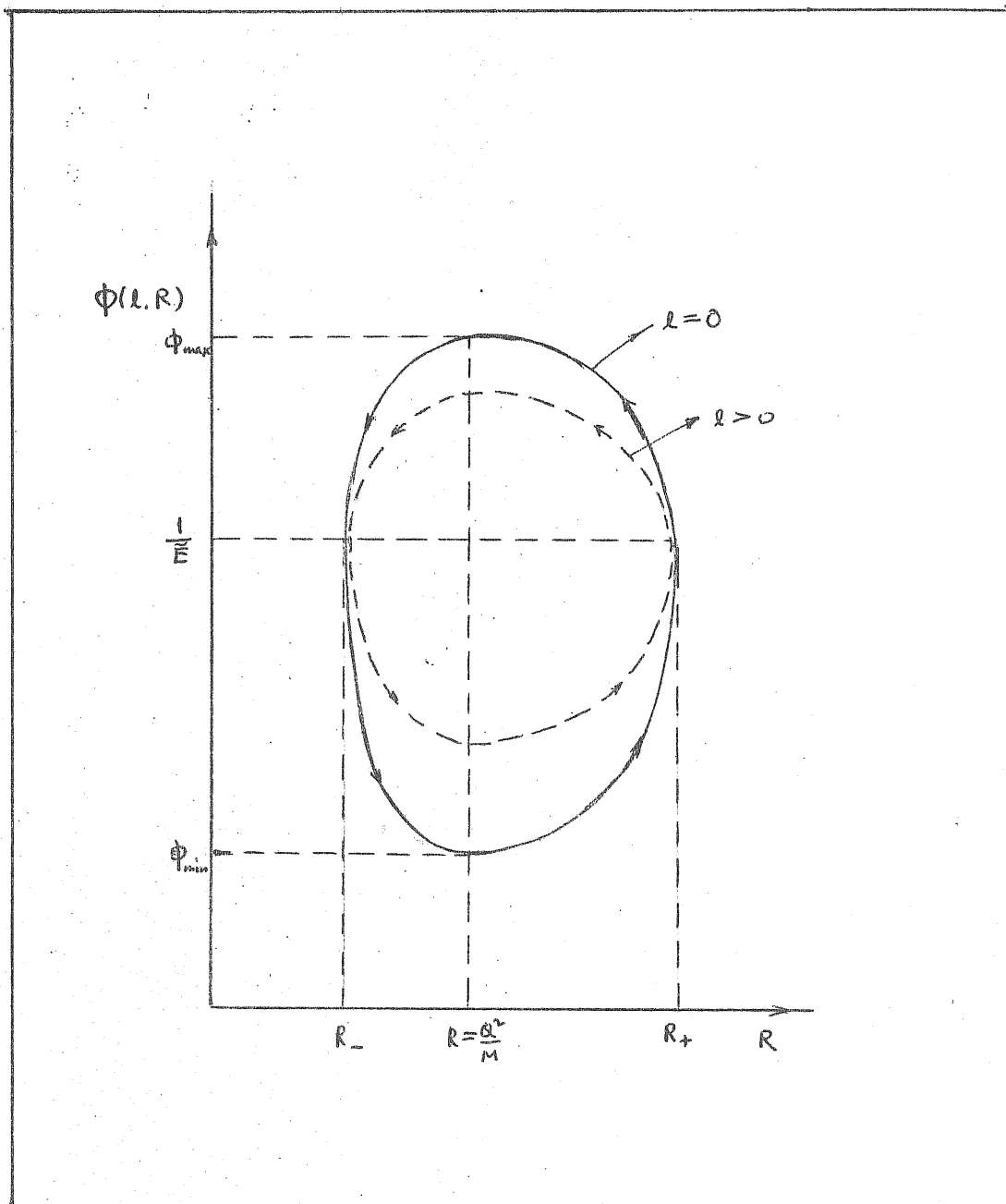


Figure 5.4 The Frequency Shift of Photons
Emitted by Vibrating Charged Stars

